2. Chemical Properties—Elemental Analysis by EDS

Amphiboles are nonstochiometric minerals and often contain substitutional cations in varying amounts. Therefore, precise determination of their chemistry is difficult and positive identification based on chemistry alone is not reliable. This may be particularly pertinent when dealing with asbestos minerals present as minor constituents in mineral samples.

Elemental ratios, which are sometimes used to distinquish between asbestos types, often vary over wide ranges even in standard samples. The presence of gold coating, which would tend to preferentially absorb x-rays from lighter elements more than heavier elements, may make the situation even worse. In view of these ambiguities, and due to inherent practical difficulties in obtaining representative quantitative EDS elemental analyses from submicroscopic fibers, the present Level II and Level III protocols specify the use of only qualitative EDS spectra, which are often very valuable for screening purposes in the identification procedure. For example, in distinguishing between tremolite and actinolite type of amphibole, actinolite usually contains Fe, but tremolite does not.

3. Selected Area Electron Diffraction (SAED)

The method of obtaining an SAED pattern of a randomly oriented specimen is usually described in the EM instruction manual. The general directions for using the instrument to obtain and photograph SAED patterns are:

(1) Select the image magnification for the selected area.

(2) Bring the desired field of view to the center of the screen.

(3) Insert the appropriate field-limiting aperture (according to the desired field of view) into the beam path.

(4) Obtain the sharpest field-limiting aperture shadow.

(5) Confirm that the desired field of view is in the field-limiting aperture.

(6) Focus the specimen image; a photograph of the selected area image can be taken.

(7) Obtain the SAED pattern, remembering to retract the objective lens aperture from the beam path. The SAED pattern will be observed on the fluorescent screen.

(8) Select the desired camera length (the shorter the length, the better for SAED patterns of asbestos taken at high magnification).

(9) Focus the SAED pattern sharply. The beam stopper is used to intercept the bright center spot.

(10) For photography, the illumination is expanded (condenser reduced) after focusing the pattern, so that the pattern becomes barely visible (indistinct). A manual time exposure of approximately 20 to 30 s (maybe more depending on such factors as specimen and film) is required. The beam stopper can be left in place or removed from the beam path 1 to 2 s before closing the shutter. A double exposure of the specimen image and the SAED pattern can be taken if particle-to-particle spacing is adequate.

4. Use of Tilting to Acquire Exact Zone-Axis SAED Patterns

Determination of the Tilt Axis—

In the side-entry type electron microscopes, the instrument tilt axis is always fixed. However, the position of the tilt axis on the viewing screen shifts with magnification. Also, there is always an angular rotation between the image and the SAED pattern. It is highly desirable to know the location of the tilt axis on the viewing screen and its relationship vis-a-vis SAED pattern under the operating conditions to make effective use of specimen tilting for obtaining exact zone-axis orientations. The following steps can be used to locate the position of the tilt axis:

(1) A gold-coated EM grid with a standard asbestos mineral specimen on a polycarbonate replica film is placed in a tilt-rotation or double-tilt holder and inserted at 0° tilt into an aligned TEM set at 100 kV, 100 μA, 20,000X magnification, and 20-μm camera length operation.

(2) The image is focused on the fluorescent screen, which is at approximately 16,000X magnification.

(3) A circular hole in the polycarbonate replica is positioned in the center of the field of view.

(4) On tilting, the circular feature changes to an ellipse with the major axis unchanged, and indicates the position (direction) of tilt axis at that magnification. The minor axis shows the perpendicular direction to the tilt axis. A high tilt angle defines the tilt axis more accurately than a small tilt angle. Figure A15 illustrates the effect of tilt.

(5) A double-exposure photograph at 0° tilt and at some high tilt angle, such as 30°, is taken of the focused circular hole for reference.

Tilting—for zone-axis SAED Patterns—

Quantitative SAED requires knowledge of crystallography to obtain useful zone axis diffraction patterns from which precise measurements can be made for comparison with known asbestos standards on file. Thus the method of obtaining the visual SAED pattern of randomly oriented specimens, as in Level I and II analysis, is modified for quantitative SAED pattern analysis. It requires tilting of the specimen to align major crystallographic directions with the

electron beam. The zone axis is a line parallel to a set of intersecting crystal planes and nearly parallel to the electron beam. A zone-axis pattern thus gives regular repeat distances and even intensities of spots throughout the pattern.

Either a double-tilt or a tilt-rotation type specimen holder can be used for obtaining zone-axis patterns. A double-tilt holder is often preferred because tilt-rotation combination involves translational movement of the fiber during tilting, necessitating constant adjustment of the specimen-positioning controls to keep the specimen centered in the SAED aperture. On the other hand, it is much easier to obtain an accurate measure of the degree of tilt and perform systematic tilting with the tilt-rotation specimen holder. It is only necessary to rotate the specimen (fiber) until the tilt axis (as determined earlier) coincides with a major row of spots and then tilt until a major zone axis is parallel to the incident electron beam. Alternately, fiber axis of the fiber can be oriented either parallel or perpendicular to the tilt axis and then further tilting is used to obtain exact zone-axis orientations.

In order to avoid flip-flopping between image and diffraction modes while tilting, a recommended procedure is to defocus the diffraction pattern (the aperature becomes visible and the specimen/fiber can be seen in it) so that a double image of fiber in aperture can be seen with a poorly focused diffraction pattern. The movement of the fiber can then be tracked in relation to the spot pattern during tilting and kept centered in the SAED aperture by use of the specimen-positioning controls (knobs) of the microscope. Sometimes a larger aperture aids in the tracking-pattern recognition process.

An experienced electron microscopist can readily recognize the geometrical features like Kikuchi lines or Laue zones in the SAED pattern and use these to obtain the exact zone-axis SAED patterns. A detailed discussion of Kikuchi patterns and Laue zones and their utility in tilting experiments may be found in any standard text book on electron microscopy. Use of the double-tilt specimen holder is very helpful and less tedious in tilting experiments. However, all laboratories may not have both types of specimen holders available. A skilled microscopist can use either specimen holder without much difficulty. Experience and skill are more important factors in SAED analysis than the type of specimen holder used.

5. Characteristics of SAED Patterns Encountered in Asbestos Analysis

Successful application and exploitation of SAED analysis in asbestos analysis needs prior knowledge of the general appearance and distinguishing characteristics of other SAED patterns which are often encountered. The following discussion summarizes some of the observed SAED features of asbestos and other related minerals. This discussion is by no means comprehensive and assumes that the reader is familiar with general crystallography and the nomenclature pertaining to varous aspects of SAED patterns.

Minnesotaite and Stilpnomelane—

These iron-rich non-asbestos layer minerals are often encountered in asbestos analysis of specimens from certain geographic locations. Particulates of these minerals lie near their basal (001) planes. Stilpnomelane and

minnesotaite both possess large superlattices and their commonly observed SAED patterns are easily distinguishable from amphibole patterns. The spacing (in reciprocal space) is about half (for minnesotaite) or less than that for most amphiboles. These minerals can be readily distinguished in Level I or Level II analyses if a gold coating (optional) is applied to the specimen grids. A visual inspection of the number of rows of spots inside the (111) gold ring is sufficient to distinguish minnesotaite and stilpnomelane from amphiboles.

Chrysotile—

Due to the cylindrical lattice of chrysotile the SAED pattern is unique. The SAED pattern observed is symmetrical about the cylinder axis, x, and the spacing of the rows of spots is proportional to 1/a, where a is 0.53 nm. The most distinguishing features of the pattern are the flared spots of the type (130) which occur in the firt layer line. The flaring is due to the cylindrical lattice. A typical EDS spectra shows the presence of only Mg and Si (Figure A11).

Amphiboles—Systematic Absences, Twinning, and Double Diffraction—

The most commonly observed row of diffraction shots found in SAED patterns in amphiboles is in the y* or b* direction, representing the shortest reciprocal spacing between the spots (18.4 Å in real space). There are many strong zone axis orientations containing the y* row of spots. The lattice of amosite, crocidolite, tremolite, and actinolite is c-centered, and for such a lattice the h + k odd spots are absent along the y* or b* row. In practice, however, weak spots may be present in forbidden positions due to the presence of thin multiple twinning on (100), which cause streaking parallel to a*. Often, reciprocal nets from both twins are present in the same SAED pattern. In a twinned crystal, the number of important diffraction nets containing b* is doubled, leading to the observation that the diffraction patterns appear insensitive to tilt.

In some cases SAED patterns can contain spots from both twin individuals which overlap. However, not all the spots present in the composite SAED patterns are generated by the overlapping nets; some spots may be present because of double diffraction where a diffracted beam from one twin becomes the transmitted beam when it enters the other twin.

The purpose of the above discussion is to point out that although many complications exist in the analysis of SAED patterns, these can be overcome; in a good goniometric tilting stage most amphiboles can be identified by SAED analysis.

Amosite—

The nearest reciprocal lattice section to the (100) direct lattice plane in amosite is (301)* and it is also the most commonly observed section. Due to the presence of the thin (100) twins, this section closely resembles (100)*.

Typical EDS spectra from amosite fibers (Figure A11) show mainly Si and Fe with smaller amounts of Mg and Mn. Mn is frequently observed as a substitutional cation in amosite.

Crocidolite—

Most of the commonly observed patterns are asymmetrical and cannot be indexed easily. However, they all show rows of spots separated by a reciprocal repeat (R) corresponding to the fiber axis (0.53 nm).

The main elements observed in typical EDS analysis are Mg, Si, Ca, and Fe. Na, which is usually present in crocidolite, may not be detected in gold-coated specimens because of absorption, or because of overlapping secondary peaks from the copper grid.

Tremolite-Actinolite—

Temolite and actinolite show a variety of SAED patterns which have very similar appearances. In actinolite some of the Mg is replaced by Fe, with the result that interplanar d-spacings of actinolite are slightly larger than tremolite. In both tremolite and actinolite, the main elemental constituents are Mg, Si, and Ca. Actinolite also contains some Fe.

Anthophyllite—

Even though anthophyllite has an orthorhombic crystal structure, its commonly observed patterns are similar to the monoclinic amphiboles. Anthophyllite fibers dehydrate more easily in an electron beam and are, therefore, more difficult to study.

EDS elemental analysis shows the main constituents to be Si and Mg with a small amount of Fe.

6. Determination of Camera Constant and SAED Pattern Analysis

As mentioned earlier, a thin film of gold is evaporated on the specimen EM grid to obtain zone-axis SAED patterns superimposed with a ring pattern from the polycrystalline gold film. Since d-spacings corresponding to identifiable gold rings are known, these can be used as an internal standard in measuring unknown d-spacings on an SAED pattern from a fiber. The precision of measurement is as good as the quality of the photograph (or negative) and usually the measurements should be in the order of 0.1-0.2 mm with an angular tolerance of 0.5-1.5 degrees. The measurements can be made by several methods: manually with a ruler, with a mechanical aid, or a densitometer, etc. The patterns can be read directly on the developed negative or on an enlarged non-glossy print.

In practice, it is desirable to optimize the thickness of the gold film so that only one or two sharp rings are obtained on the superimposed SAED pattern. Thicker gold film would normally give multiple gold rings, but it will tend to mask weaker diffraction spots from the unknown fibrous particulates. Since the unknown d-spacings of most interst in asbestos analysis are those which lie closest to the transmitted beam, multiple gold rings are unnecessary on zone-axis SAED patterns.

7. Determination of Camera Constant Using Gold Rings

An average camera constant using multiple gold rings can be determined as explained below. However, in practice, in most cases determination of the

average camera constant is not necessary and thicker gold films are not desirable. The camera constant, CC, is 1/2 the diameter, D, of the rings times the interplanar spacing, d, of the ring being measured and is expressed as:

$$CC(\text{mm-Å}) = \frac{D(\text{mm})}{2} \times d(\text{Å})$$

The value of d for each ring can be obtained from the JCPDS file.

(a) Measure the diameters (two perpendicular locations) of the gold rings in mm as precisely as possible (see Figure A16).

(b) Measure as many distinct rings as possible to minimize systematic errors.

(c) Example: if the measured values in mm are D_1, D_2, D_3, D_4, and D_5, these will represent, respectively, d-spacings of

$$\frac{4.079}{\sqrt{3}}, \frac{4.079}{2}, \frac{4.079}{\sqrt{8}}, \frac{4.079}{\sqrt{11}}, \text{ and } \frac{4.079}{\sqrt{12}} \text{ Å}$$

(d) The camera constants will be:

$$CC_1 = \frac{D_1}{2} \times \frac{4.079}{\sqrt{3}} = \frac{D_1}{2} \times 2.355$$

$$CC_2 = \frac{D_2}{2} \times \frac{4.079}{2} = \frac{D_2}{2} \times 2.04$$

$$CC_3 = \frac{D_3}{2} \times \frac{4.079}{\sqrt{8}} = \frac{D_3}{2} \times 1.442$$

$$CC_4 = \frac{D_4}{2} \times \frac{4.079}{\sqrt{11}} = \frac{D_4}{2} \times 1.23$$

$$CC_5 = \frac{D_5}{2} \times \frac{4.079}{\sqrt{12}} = \frac{D_5}{2} \times 1.178$$

(e) The camera constant for the SAED pattern is the average of CC_1, CC_2, CC_3, CC_4, and CC_5. Table 2 presents an example of camera-constant determination.

TABLE 2. DETERMINATION OF CAMERA CONSTANT (EXAMPLE)

Ring No.	D_i readings (mm)	Mean D_i (mm)	d-spacing, d_i (Å)	Camera constant $C_i = D_i/2 \times d_i$
1	23.0, 22.0	22.5	2.355	26.5
2	27.4, 27.6	27.5	2.04	28.0
3	37.8, 38.2	38.0	1.44	27.4
4	44.6, 45.4	45.0	1.23	27.7

Mean Value of Camera Constant $= \frac{\Sigma C_i}{n} = \frac{26.5 + 28.0 + 27.4 + 27.7}{4} = 27.4$ (mm-Å)

8. Measurement of d-Spacings and Interplanar Angles

The gold film, because of its small, randomly oriented crystallites, produces a ring pattern superimposed on the SAED pattern from the fibers. The diameters of the gold rings correspond to known values of d-spacings, and this provides an internal standard to correct for inherent uncertainties present due to variations in instrumental and/or operating conditions. Since the d-spacings of interest on SAED patterns are usually the ones that lie closest to the center spot (transmitted beam), a camera constant measured from the first gold ring in the direction of measurement of d-spacings will usually give better accuracy in computed spacings than the use of an average camera constant. This method will account for any distortions in the symmetry of the gold ring pattern. The zone-axis SAED pattern usually has several rows of spots within the circular pattern of the gold rings. These rows of spots contain information about the two sets of planes in the crystal structure and the angle between them. The following procedure outlines the steps necessary to obtain the distances between planes (d-spacings) and the corresponding interplanar angle, θ (see Figure A17):

(1) From the spot pattern, determine the row with spots most closely spaced, and designate this as a horizontal row. Draw a fine line to show the row through the origin, and designate this the zeroeth row. Draw fine lines to show the first and succeeding horizontal rows. For a few horizontal rows, measure the mean spacing between adjacent spots (or the minimum vector):

$$X_i = \frac{\text{Distance between spots m units apart}}{m}$$

where m is chosen as an optimum number to minimize measurement errors. The mean horizontal spot distance, X,

equals the summation of X_i divided by the number, n, of rows measured. The d-spacing in Å corresponding to this vector is the camera constant divided by X, and is labeled d_2. Table 3 presents an example of spot spacing measurement within a horizontal row.

(2) The perpendicular distance between two adjacent horizontal rows is similarly measured. This interrow spacing, Z, is the mean separation between horiziontal rows, and equals the distance between a number of rows divided by the number of spaces. This distance is an additional vector for comparison that coincides with the slant vector, d_1-spacing, when angle $\theta_{1,2}$ is 90°. The row-spacing (R) equals the camera constant divided by Z. Table 3 presents an example of perpendicular spacing between horizontal rows; Figure A17 illustrates spot and row spacing.

(3) To obtain the d_1-spacing and corresponding angle $\theta_{1,2}$, a perpendicular is drawn to the zeroeth horizontal row through the origin. A line is drawn to the first spot to the right of the perpendicular in the first row and extended through the succeeding rows. This line, called the slant vector, forms the acute angle $\theta_{1,2}$. The mean spacing, Y, between spots on the slant vector can be measured by dividing the maximum distance between spots by the number of spaces between them, or by calculating from the interrow spacing:

$$Y = \frac{R}{\sin \theta_{1,2}}$$

The d-spacing in Å corresponding to this vector is the camera constant, CC, divided by Y and labeled d_1.

$$d_1(\text{Å}) = \frac{CC \times \sin \theta_{1,2}}{R} = \frac{CC}{Y}$$

Figure A18 illustrates the relationship of d_1, d_2, $\theta_{1,2}$ and R. In some cases, the interplanar angle $\theta_{1,2}$ may be more than 90 degrees (not shown in Figure A18).

Summary of Data from Each SAED Pattern:

(a) The camera constant, CC, as determined from the gold rings, normalizes the distances on the SAED pattern regardless of such factors as magnification and tilting.

TABLE 3. DETERMINATION OF SPOT SPACINGS (EXAMPLES)

Reading	Separation (mm)	Units	Mean spacing, X_i (Å)
Spot spacing within a horizontal row, d_2:			
1	49	16	3.006
2	42.7	14	3.05
3	—	—	—
			3.028 = Mean

$$\text{d-spacing} = \frac{27.4}{3.028} = 9.05 \text{ Å}$$

Perpendicular spacing between horizontal rows, R:

1	43	8	5.0375
—	—	—	—
—	—	—	—
			5.0375 = Mean

$$\text{d-spacing, R} = \frac{27.4}{5.0375} = 5.44 \text{ Å}$$

Note: It is preferable that the camera constant values used in computing d-spacings are measured from the first one or two gold ring diameters in the direction of d-spacing measurement.

(b) The parameters of interest are:

- d-spacing of spots in a horiziontal row: $CC/X = d_2$
- d-spacing of spots in the slant vector: $CC/Y = d_1$
- angle $\theta_{1,2}$ formed between a horizontal row and slant vector
- d-spacing corresponding to row separation as an additional parameter of interest: $CC/Z = R$.

It should be noted that the use of camera constant in the form used here in calculating d_1, d_2, and R, which are measured in reciprocal space on SAED patterns, automatically converts the calculated numbers into real space spacings, which are then compared to those from a suitable standard file.

9. Identification of Unknown Fibers

Unknown d-spacings (d_1 and d_2), interrow spacing (R), and interplanar angles (θ) measured from zone-axis SAED patterns of unknown fibers are compared with corresponding known values tabulated in JCPDS powder diffraction files, or those computed using lattice parameters and crystal structures of candidate asbestos minerals, or with the values contained in an internally developed file from standard specimens of candidate minerals. Table 4 is an example of the IITRI standards file (Jones et al., 1981). Figures A19 to A22 are examples of zone-axis SAED patterns.

Unknowns are matched as closely as possible to the file parameters for positive identification. However, considerable care and competent judgment are required in Level III confirmatory analysis. For example, amphiboles are usually nonstochiometric minerals, and thus a perfect match may not be possible between the d-spacings and interplanar angles determined from unknown fibers and those available from standard minerals. JCPDS Powder Diffraction files do not list interplanar angles. Since amphiboles have low-symmetry crystal structures, tabulated values of d-spacings and interplanar angles would be extensive and very expensive to generate, and to get an accurate match may not be possible because these tables are derived assuming certain lattice parameters which may not be the same as those of the unknown fibers being analyzed. Given these inherent uncertainties, it would seem that use of internally developed SAED files consisting of several readily accessible orientations (by virtue of natural habit of amphibole fibers) from standard amphibole species could eliminate a lot of tedious unnecessary work and yet provide reliable data for comparison and identification of unknown fibers.

In practice, SAED analysis combined with qualitative EDS analysis may help resolve certain cases where a close match in d-spacings and interplanar angles is not possible. For difficult specimens or SAED patterns of controversial nature, a second opinion may be necessary, especially if a legal case is involved.

TABLE 4. COMPARISION OF d-SPACINGS FROM SAED FILE AND POWDER DIFFRACTION FILE (EXAMPLE)

Amphibole type	Zone axis	Internal Standard File Data				Powder Diffraction File Data (1975)		
		d_1 (Å)	d_2 (Å)	θ (deg)	Interrow spacing, R (Å)	d_1 (Å)	d_2 (Å)	File index no.
Amosite	[100]	5.3	9.14	90.0	5.3	5.22	9.20	17-725
	[30$\bar{1}$]	1.79	9.26	84.0	—	1.76	9.20	17-725
	[101]	4.88	9.23	74.0	5.17	4.84	9.20	17-725
	[$\bar{1}$01]	4.14	9.11	78.0	4.21	4.10	9.20	17-725
	[$\bar{3}$10]	5.22	5.13	95.0	—	5.22	5.12	17-725
Crocidolite	[100]	5.22	8.97	90.0	5.22	5.20	9.02	19-1061
	[101]	4.94	9.05	75.0	5.19	5.89	9.02	19-1061
	[$\bar{1}$10]	4.79	8.19	79.0	5.23	4.89	8.40	19-1061
	[30$\bar{1}$]	1.75	8.97	83.5	—	1.76	9.02	19-1061
	[$\bar{3}$10]	5.12	5.12	96.0	—	—	—	19-1061
Tremolite	[100]	5.04	9.03	90.0	—	5.07	8.98	13-437
	[101]	4.83	9.03	75.0	—	4.87	8.98	13-437
	[$\bar{2}$0$\bar{1}$]	2.59	8.97	80.5	—	2.59	8.98	13-437
	[30$\bar{1}$]	1.72	8.98	83.5	—	1.69	8.98	13-437
Anthophyllite	[100]	—	—	90.0	5.24	5.28	8.90	9-455
	[$\bar{1}$42]	4.56	4.56	60.0	—	4.50	4.50	9-455

SECTION 7

ARCHIVAL SAMPLES

DISCUSSION OF PROTOCOL

Samples that have been collected on filter substrates other than polycarbonate, or that have been collected without regard to filter loading levels, are referred to as archival samples. These samples were usually collected for other analytical objectives, such as for optical microscopy or gravimetric analysis, for defined sampling periods without regard to concentration levels in the air, or for collection of particles larger than 10 μm in diameter. Such samples were historically collected, and are of value and interest in determining the presence of asbestos fibers and/or structures. Filter substrates designated as archival samples include glass fiber filters; cellulose or modified paper filters; cellulose ester filters; other organic polymeric membranes, such as polystyrene, nylon, and polyvinyl chloride; and all overloaded organic polymeric membrane filters.

The purpose of the preparation step is to transfer particles from a filter surface to an EM grid with a minimum of distortion in morphology and size distribution. The nature of non-polycarbonate filter substrates or particle loading makes it sometimes necessary to transfer a satisfactory quantity of particles to a polycarbonate filter prior to transfer to the EM grid. At present, only transfer to an EM grid from a polycarbonate filter has been standardized.

A modified preparation technique is recommended for archival samples, followed by the analytical methodology using Level I, Level II, or Level III effort--with the understanding that these samples will indicate the presence of asbestos, and secondarily the number, size, distribution, and morphology. The results from sample to sample are less precise due to problems in standardizing the preparation procedures used for archival samples.

The archival filter samples are prepared for analysis based on the information sought, type of filter material, and particle loading on the filter. The various preparation techniques for these filters include:

(1) Individual particle picking and/or reverse washing of the filter, with subsequent filtration of the filtrate using a polycarbonate filter.

(2) Collapsing the membrane filter structure by exposure to solvent vapor (surface fusion), to produce a more uniform substrate for replication and grid transfer.

(3) Solubilizing filter material in selected solvents, followed by separation of particulates.

(4) Low temperature ashing (LTA).

Two preparation methods are recommended based on filter loading and type of filter material: surface fusion, and LTA.

DESCRIPTION OF METHODOLOGY

Because the greatest number of archival samples have cellulose ester substrates, this type of filter material is used in examples describing the methodology.

1. Samples with Adequate Loading

Discussion—

As an example, samples collected on cellulose ester filters have been received by a laboratory. Direct transfer of the particulates to the EM grid is possible using acetone as the solvent in a modified Jaffe wick washer. However, a question arises concerning indeterminate particle loss in the transfer. Carbon-coating the cellulose ester filter prior to grid transfer minimizes particle loss. However, this improvement in particle count is offset by difficulty in visually observing and counting the fibrous particles against a replica background of the uneven surface topography of the cellulose ester filter, and by indeterminate loss of very small particles hidden in the crevices of the uneven filter surface. The NIOSH method of surface fusion (Zumwalde and Dement, 1977) is relatively reliable, and produces a more consistent result, although the question of loss of the very small particles has not been resolved. LTA, described later in this section, may also be used for these samples.

Procedure—

The NIOSH technique, a modification of a particle-transfer technique developed at Los Alamos Scientific Laboratory (Ortiz and Isom, 1974), is described as follows:

(1) A section of the membrane filter is cut with a scalpel, and placed on a clean microscope slide with the sampled side facing up.

(2) The cut section is fastened on all sides to the slide with narrow strips of transparent tape.

(3) The slide, with the cut section, is exposed to acetone vapor (not liquid) for approximately 10 min. The acetone vapor collapses the structure of the filter and produces a fused, relatively smooth-surfaced film. The size of the acetone vapor bath and time of filter response to the vapors are critical in obtaining the desired smooth, fused surface; each laboratory must determine its own optimum conditions.

(4) The fused filter section is placed on the rotating stage of the vacuum evaporator for carbon-coating.

(5) A 3-mm-diameter portion of the carbon-coated filter is transferred to a carbon-coated EM grid in the modified Jaffe wick washer.

(6) Acetone is used in dissolving the fused membrane filter.

(7) Transfer to the grid and options for analytical efforts were described previously.

2. Samples with Heavy Loading

Discussion—

As an example, samples collected with a heavy deposit of particulates have been received by a laboratory. These particulates may be organic in nature (for example, pollen or soot), or of mineral matter. LTA is used to remove the organic material (filter as well as particulates), leaving the inorganic residue. The residue is gently resuspended and dispersed in filtered distilled water by low-wattage, short-time ultrasonification. The resuspension is then filtered onto a 0.1-μm (pore size) polycarbonate filter. The dry, particulate-loaded polycarbonate filter is then carbon-coated and transferred to EM grids for analysis as described previously.

Low temperature ashers are available with one, two, or four chambers. The following modifications minimize contamination in using these units:

(1) A single chamber is dedicated for ashing samples for EM analysis.

(2) An in-line filter is placed in the oxygen supply between the regulator and entry into the asher.

(3) For models with direct access to ambient laboratory air on completion of ashing and return to ambient pressure, a filter is placed in the inlet line to prevent laboratory air from being sucked into the chamber.

In using the single-chamber method, a blank test tube and the sample tubes (up to four, for a total of five in a 10-cm-diameter chamber) are placed in the chamber lengthwise, with the opening facing the door.

The filtration step is also used in diluting the initial heavy particulate loading. Filtration of aliquots is not recommended to obtain different levels of loading on the new filters; a representative sample from each aliquot in the filtration of suspensions is difficult to obtain. Instead, for heavy loadings, different known areas of filter segments (one-eighth, one-fourth, or one-half of the filter) should be ashed so that the entire contents of the resuspension tube can be filtered onto either a 25-mm-, 37-mm-, or 47-mm-diameter polycarbonate filter for the desired dilution.

Distilled water is filtered through a 0.1-μm (pore size) polycarbonate filter prior to use. All glassware is washed with soap and water, rinsed with acid, and then rinsed with particle-free distilled water. The dedicated asher chamber is carefully wiped with damp lens paper.

LTA Procedure—

The LTA manufacturer's instructions are followed since the power required for one, two, or four chambers, the mass (glassware plus sample) placed in the chamber, and the desired rate of ashing all vary. In general, the following steps are performed:

(1) Each filter segment with a known deposit area is carefully placed in a clean test tube (13 mm x 80 mm) using a clean tweezer.

(2) With forceps, the tubes containing the sample, and one lab blank (unused filter segment of the same size and type of filter material as the sample) are placed lengthwise, side by side in the chamber, with the mouths of the tubes facing the open end (door) of the asher chamber. The tubes are laid in the center of the chamber within the region of the coils surrounding the chamber. Up to four sample tubes and one blank can be laid like logs inside the chamber.

(3) The power is slowly and carefully increased to prevent "flashing" of the filter, which would result in loss of sample.

(4) The filter membrane vanishes in about 30 min; ashing is continued for another 2 to 3 h to ensure complete ashing. The chamber is slowly allowed to reach ambient pressure.

(5) The test tubes are carefully removed and placed in a beaker, covered, and stored on a class-100 clean bench for resuspension.

Resuspension (Sonification) Procedure—

Ultrasonification is used in resuspending and redispersing the ash resulting from the LTA. The superiority of a probe-type ultrasonic device over a bath-type device has not been demonstrated. However, the criteria of low energy and minimum sonification time appear valid. The probe-type instrument is more readily calibrated (desired reproducibility), but requires a larger volume of suspension to work with. The bath-type instrument is more difficult to calibrate, and is usually of fixed wattage. A generalization is that probes are used for dispersing, baths for cleaning. Recently, a bath-type ultrasonic unit (Ladd Research Industries, Inc., Burlington, Vermont) with a variable power source and timer has become available that appears to have the advantages of both types of ultrasonic devices.

The resuspension procedure is as follows:

(1) 10 mL of filtered distilled water is added to each test tube.

(2) Each tube is placed in a 100-mL beaker containing 50 mL of water.

(3) The beaker, with the tube, is placed in the low-energy ultrasonic bath.

(4) Ultrasonic energy of about 50 to 60 W (60%) is applied for 3 min.

Filtration Procedure—

Liquid filtration of suspensions for EM examination using polycarbonate filters is one of the more difficult procedures to standardize. Variations in the nature of the filter material, geometry and distribution of pores, and method of manufacturing make it difficult to obtain a uniform deposit of particulates on the filter. The following procedure is used for consistency in the filtration procedure:

(1) A filtering apparatus having a filter size adequate for the desired dilution--preferably 25-mm or 47-mm diameter—is assembled. A polycarbonate filter (0.1-μm pore size) is used shiny side up for the deposit, with a cellulose ester filter (5-μm pore size) as a backing filter on the glass frit.

(2) While dry, the filters are centered and suction is applied. The filter funnel is mounted on the centered, perfectly flat filters with the vacuum on.

(3) The vacuum is then turned off. A 2 mL amount of particle-free distilled water is added to the filter funnel, followed by careful addition of all the water in the test tube containing the dispersed ash. The test tube is rinsed twice with particle-free distilled water, and the contents are carefully added to the filter funnel.

(4) Suction is then applied; neither rinsing the filter funnel nor adding extra liquid is permitted during the entire filtration process.

(5) At the end of filtration, suction is stopped.

(6) If possible, the filter is dried on a glass slide or holder that can be placed directly in the vacuum evaporator for carbon-coating.

(7) The dry filter is stored in a disposable Petri dish (taped on a glass slide), or in the special holder, until ready for carbon-coating, grid transfer, and EM analysis.

(8) The effective area of the redispersion filter and the area of original filter deposit cut for ashing must be recorded (ashing factor) for inclusion in analytical data reduction and reporting.

SECTION 8

BULK-SAMPLE ANALYSIS

DISCUSSION OF PROTOCOL

Bulk samples may be air samples collected in large volumes using electrostatic precipitators, bag collectors, or high-volume samplers, for example; or they may be original pieces of source material containing asbestos, such as insulation, asbestos paper products, and asbestos cement products.

Efficient usage of the three levels of analysis requires effective communication between those requesting an analysis and those responsible for conducting the analysis. Personnel requesting an analysis must understand the limitations of each level of analysis by EM. For example, requesting EM analysis of a bulk-material (solid) sample, where there is marked disagreement regarding the presence of asbestos (amphibole), and using Level I (screening) analysis, are incompatible. Bulk-material samples require grinding for analysis; grinding requires care to minimize such problems as contamination, change in size of the asbestos fiber, increase in fragments that morphologically meet the criteria of a fiber, possible change in the relationship of asbestos to nonasbestos components, and possible destruction of asbestos fiber crystallinity.

Following grinding, bulk-material samples should first be analyzed by PLM, followed by XRD, if necessary. XRD provides information on samples having asbestos concentration levels of at least 2%. PLM provides information on asbestos and nonasbestos components, as well as on the size of the asbestos fibers in the solid-bulk phase. The additional information aids in EM analysis of these samples at the selected level of analysis.

DESCRIPTION OF METHODOLOGY

1. Polarized Light Microscopy

Analysis of bulk samples, such as insulation material, for component identification and for determination of the type and concentration of asbestos present is best accomplished by PLM. With the polarized light microscope, particle properties--such as color, morphology, refractive index, birefringence (which indicates a crystalline substance rather than an amorphous substance), surface texture, reflectivity, and magnetism--can be observed and determined. Determination of such a large number of particle properties allows identification of specific particle types, in most cases. For example, amorphous slags and crystalline minerals are common nonfibrous filler components of insulation materials that can be easily distinguished by PLM.

2. X-Ray Diffraction Analysis

XRD has been successfully used to measure asbestos content in both aerosol samples and bulk samples. The reported values for sensitivity and accuracy vary depending on the exact technique, but recent reports quote sensitivity values of about 1% chrysotile, whereas 5% was more common when the technique was first demonstrated. Much of the improved sensitivity derives from sample preparation techniques, which are important in XRD, but digital data collection and use of such accessories as x-ray monochromators to reduce background are also important.

While 1% sensitivity has not been demonstrated for asbestos materials other than chrysotile, the same sample preparation procedures are applicable to other mineral forms, with comparable sensitivities expected in cases with serious interfering lines. Interferences would hinder the analysis for chrysotile as well as for other asbestos minerals. Considering that the high-sensitivity procedures have been only partially demonstrated at the 1% level, a sensitivity of, say, 2% is probably a more realistic expectation for asbestos minerals in general.

3. Electron Microscopy

For bulk-air samples, asbestos analysis by EM entails an addition to the sample preparation procedure to attain a representative powder sample at a suitable concentration level to be placed on the EM grid. This additional step is similar to the method used in preparing standards of known asbestos. The finely divided powder samples are split into representative fractions, and a small, weighed portion is suspended in a known volume of filtered distilled water containing 0.1% Aerosol OT.* A mild ultrasonic treatment is used to disperse the particles. Different known volumes of suspension are filtered through a 0.1-μm (pore size), 25-mm-diameter Nucleporet membrane filter. The dried Nuclepore filter is then carbon-coated and transferred to an EM grid using the refined Jaffe wick technique described previously.

Bulk-solid samples are gently and slowly ground to a powder for EM analysis to minimize localized heating; the powder is then prepared for the EM grid by the method described for bulk-air samples.

For EM analysis of bulk-air samples, a weighed portion is suspended in filtered distilled water, deagglomerated in an ultrasonic bath, transferred to a volumetric flask, and brought to volume with filtered distilled water. An aliquot is then filtered onto a 0.1-μm (pore size) polycarbonate filter using a 5.0-μm (pore size) cellulose ester filter as a back-up filter on the filtration apparatus. The dried polycarbonate filter is then carbon-coated. A 3-mm x 3-mm portion of the carbon-coated filter is then directly transferred to a 200-mesh carbon-coated copper EM grid using the refined Jaffe wick washer technique. EM analysis based on Level I, II, or III effort is then performed.

---

* Fisher Scientific Co. (Cat. no. 50-A-292), 711 Forbes Ave., Pittsburgh, Pa.

† Nuclepore Corporation, 7035 Commerce Circle, Pleasanton, Calif.

SECTION 9

NUMERICAL RELATIONSHIPS AND ANALYTICAL AIDS

The fibrous structures (fibers, bundles, clusters, and matrices) in an air sample are to be counted, sized, and identified as asbestos or non-asbestos. An air sample ranging from 1 to 5 m^3, depending on its total suspended particulates (TSP) content (in ambient air, the average TSP is between 30 and 300 $\mu g/m^3$) is drawn through a 37-mm filter (effective filtration area of 8.6 cm^2) or a 47-mm filter (effective filtration area of 9.6 cm^2). The asbestos content, unlike a prepared laboratory standard or sample, is a very small percentage (less than 1%) of the particulate loading (TSP content) collected on the filter surface.

Two small circular sections of the filter of approximately 3-mm diameter are transferred to EM grids for transmission electron microscopy. Either one or both EM grids are examined for asbestos content; 10 random grid openings are examined for each EM grid. Each grid opening measures approximately 85 µm x 85 µm. At 20,000X magnification, a field of view of 4.5 µm x 5.0 µm is used in the examination. This approximates to about 300 fields per grid opening or 3000 fields of view per grid examined (6000 fields for two EM grids) if less than 100 asbestos structures had been found. Unlike a field blank or laboratory blank, the statistical significance of obtaining a low asbestos count in the midst of atmospheric clutter needs to be recognized.

LIMITS OF DETECTION

The minimum detection limit of the EM method for counting airborne asbestos fibers varies depending on the amount of total extraneous particulate matter in the sample, and on the contamination level in the laboratory environment. This limit also depends on the air sampling parameters, loading level, and EM parameters used. For example, assuming that a fiber count has an accuracy of ±1 fiber, when 10 full-grid openings are scanned, each grid opening having an average area of 0.72×10^{-4} cm^2, the detection limit is determined from the equation

$$\text{Detection limit} = \frac{1}{10} \times \frac{\text{Area of filter } (cm^2)}{0.72 \times 10^{-4}\ (cm^2)} \times \frac{1}{\text{Volume of air } (m^3)}$$

The minimum detection limit, then, is lower for very dilute samples. Examining full-grid openings leads to a lower value of the minimum detection limit because of the large area scanned, as compared with the field of view method. With a given sample, the detection limit can be lowered considerably, but the required experimental effort increases. The guideline of using 10

full-grid openings represents a judicious compromise between a reasonable experimental effort and a fairly low value of the detection limit. However, using two or more TEM grids reduces the detection limit further and improves the precision of the estimates.

STATISTICAL METHODOLOGY

Several statistical strategies have been used to characterize airborne asbestos distributions and estimate the abundance of asbestos fibers in a given sample. These methods range from simple tabulation of observed frequencies of fibers across grid opening samples to the fitting of statistical probability distribution such as the Poisson. This statistical section outlines a general methodology for fitting observed data to a statistical probability distribution (either Poisson or normal depending on the fit of the former). The mean and 95% confidence interval are then estimated and used for the purpose of sample description and drawing inference regarding the abundance of airborne asbestos fibers in the environment in which the samples were obtained.

As an illustration, consider the hypothetical data in Table 5.

The expected number of grid openings with no fibers is:

$$Ne^{-\hat{u}} = (98)\ (e^{-3.0204}) = 4.7806$$

The expected number of grid openings with 1, 2, 3, ... fibers are found by multiplying $Ne^{-\hat{u}}$ by $\hat{u}/r$, i.e., 4.7806 x 3.0204, 4.7806 x 3.0204/2, 4.7806 x 3.0204/3, successively.

To test the fit of the Poisson distribution to the observed data we compute a chi-square statistic, $\chi^2 = \Sigma$ (observed - expected)^2/expected = 8.26.

Since there are nine different observed frequencies (i.e., numbers of fibers) there are 9 - 2 = 7 degrees of freedom (since we estimate one parameter). The probability of $\chi_a^2 = 8.26$ is p = 0.4; therefore, we conclude that the Poisson distribution fits the observed data.

In certain cases, the observed frequencies will not have a Poisson distribution (as determined by the previously described chi-square statistic). In this case we estimate the mean (X), variance S^2, and 95% confidence limits

TABLE 5. HYPOTHETICAL DATA

No. of fibers on grid 1 opening (r)	Observed* frequency (f)	Expected frequency		Observed - expected	Probability (r)
0	3	4.78		-1.78	.049
1	17	14.44		+2.56	.149
2	26	21.81		+4.19	.224
3	16	21.96		-5.96	.224
4	18	16.58		+1.42	.168
5	9	10.03		-1.02	.101
6	3	5.04		-2.04	.050
7	5	2.18		+2.84	.022
8	0	0.82			
9	1†	0.27	1.20	-0.20	.003
10	0	0.08			
11 or more	0	0.03			
Total	98	98.0			

* The number of grid openings showing that number of fibers.

† We combine adjacent frequencies to get a minimum of 1 fiber per group. Assuming a Poisson distribution, the mean is $\hat{u} = \Sigma fr/\Sigma f = 296/98 = 3.0204$. That is, the sum of the product of the observed frequencies and number of fibers divided by the sum of the frequencies.

assuming normality. The 95% confidence limits are computed as a function of the sample variance and t distribution.

$$S^2 = \frac{n \sum_{i=1}^{k} X_i^2 - [\sum_{i=1}^{n} X_i]^2}{n(n-1)}$$

where k is the number of grid openings, n is the total number of fibers found, and X_i is the number of fibers found in grid opening i.

The 95% confidence limits are given by

$$\bar{X} \pm \frac{ts}{\sqrt{n}}$$

where t is the value of the two-tailed t distribution for probability $p < .025$ and n - 1 degrees of freedom.

1. 95% Confidence Limits for a Poisson Variate

To generate a level of confidence regarding our estimate of the number of asbestos fibers per grid opening, a 95% confidence limit can be derived. For counts of 0 through 20, Table 6 may be used.

For example, if out of 20 grid openings 15 fibers are found, the 95% confidence limits are obtained by taking the lower and upper bounds from Table 6 as 8.40 and 24.74. Then per grid opening, the 95% confidence limit is 8.40/20 to 24.74/20, or 0.42 to 1.237 fibers per grid opening.

For counts greater than 20, a simple normal approximation is computationally convenient. The normal approximation is $\lambda = L \pm \chi^* (S_L)$ where L is the observed count, S_L is $\sqrt{L}$, and χ^* is 1.96 or 2.58 for the 95% or 99% confidence limits, respectively.

For example, if 35 fibers were observed from inspection of 20 grid openings, $L = 35$, $S_L = \sqrt{35} = 5.91$, $\lambda = 35 \pm 1.96\ (5.91) = 23.4$ to 46.6 or 23.4/20 = 1.38 to 46.6/20 = 2.74 fibers per grid opening.

2. Comparison of Two Poisson Variates

In certain cases, a new test sample is compared to a "blank" or "control" sample. Table 7 gives those differences between control and test samples that are significant at the 5% level.

Inspection of Table 7 reveals that the minimal detectable difference between test and control samples is 5 fibers in the test sample and 0 fibers in the blanks. Typically, inspection of 20 grid openings for a blank control reveals between 0 and 5 fibers. At the upper bound (i.e., 5 fibers in a

TABLE 6. 95 PERCENT CONFIDENCE LIMITS

No. of Fibers	95% Limits	
	Lower	Upper
0	0.000	3.69
1	0.0253	5.57
2	0.242	7.22
3	0.619	8.77
4	1.09	10.24
5	1.62	11.67
6	2.20	13.06
7	2.81	14.42
8	3.45	15.76
9	4.12	17.08
10	4.80	18.39
11	5.49	19.68
12	6.20	20.96
13	6.92	22.23
14	7.65	23.49
15	8.40	24.74
16	9.15	25.98
17	9.90	27.22
18	10.67	28.45
19	11.44	29.67
20	12.22	30.89

TABLE 7. CONTROL AND TEST SAMPLE DIFFERENCES

Fiber Count		Fiber Count	
Control	Test sample	Control	Test sample
	1	6	21
	2	6	22
	3	7	23
	4	7	24
0	5	7	25
0	6	8	26
0	7	8	27
1	8	9	28
1	9	9	29
1	10	10	30
2	11	10	31
2	12	10	32
3	13	11	33
3	14	11	34
3	15	12	35
4	16	12	36
4	17	13	37
5	18	13	38
5	19	13	39
5	20	14	40

control sample), 18 fibers in the test sample are required for statistical significance. This estimate of 18 fibers may prove useful for establishing an asbestos detection limit criterion.

MAGNIFICATION CALIBRATION

The following steps should be performed to calibrate the magnification of the EM:

(1) Align the EM using the manufacturer's instructions.

(2) Insert mag-calibration grating replica* (with 54,864 lines per inch, or 2160 lines per mm) in the specimen holder.

(3) Switch on the beam, obtain the image of the replica grating at 20,000X magnification (or at the magnification at which the asbestos samples will be analyzed), and focus.

(4) If the fluorescent screen has scribed circles of known diameters, align one line tangentially to the circumference of one circle using stage control. Count the number of lines in a diameter perpendicular to the lines. In most cases, the other end of the diameter will be between the n^{th} and $n^{th} + 1$ line. The fractional spacing can be estimated by eye. Alternatively, the separation between lines can be estimated using the scribed circles.

(5) If X line spacings span Y mm on the fluorescent screen using this grating replica, the true magnification, M, is given by

$$M = \frac{Y \times 2160}{X}$$

The readings should be repeated at different locations on the replica, and the average of about six readings should be taken as the representative or true magnification for that setting of the EM, as in the following example:

* For example, Cat. no. 1002, E. F. Fullam Co., Schenectady, N.Y.

Line Spacings, X	mm on Screen, Y	Magnification, M
9.5	83	18871
9.3	80	18580
7.0	60	18514
8.8	80	19636
9.0	80	19200
9.0	80	19200
		Average: 19000

On most EM's with large (18-cm diameter) fluorescent screens, the magnification is substantially constant only with the central 8- to 10-cm-diameter region. Therefore, calibration measurements should be made within this small region and not over the entire screen.

PREPARATION OF BLANKS

Even after taking the utmost precautions to avoid asbestos contamination, the possibility of some contamination cannot be ruled out. Contamination should be checked periodically by running field blank samples in addition to laboratory blanks. Field blanks should be analyzed prior to laboratory blanks. A blank sample may consist of a clean filter subjected to all the processing conducted for an actual air sample. This processing may include ashing, resuspension, redeposition, carbon-coating, transfer to a TEM grid, and TEM examination.

When analyses of blank samples show significant backg: d levels of asbestos, these should be subtracted from the values obtain for field samples. Also, the minimum detection limit may be calculated as twice or three times the standard deviation of the blank or background value.

USE OF COMPUTERS

Data reduction is facilitated by computers. Computer printouts can be used in reports. Each laboratory should develop software suitable for its needs as well as to maintain basic information, such as fiber, areas examined, volume/mass of sample, and size distribution, for possible interlaboratory comparison.

Appendixes B and C present sample printouts from Level I and Level II analyses, respectively.

REFERENCES

Anderson, C. H., and J. M. Long. 1980. Interim Method for Determining Asbestos in Water. EPA-600/4-80-005, U.S. Environmental Protection Agency, Athens, Georgia. 44 pp.

Hileman, B. 1981. Particulate Matter: The Inhalable Variety. Environ. Sci. Technol., 15(9):983-986.

John, W., and G. Reischl. 1980. A Cyclone for Size-Selective Sampling of Ambient Air. APCA Journal, 30(8):872-876.

Jones, D. R., S. C. Agarwal, and J. D. Stockham. 1981. Asbestos Analysis of Iron Ore Beneficiation Plant Samples. Final Report, Work Assignments No. 3 and No. 9, Contract No. 68-02-2617. U.S. Environmental Protection Agency, Research Triangle Park, North Carolina. 228 pp.

Leidel, N. A., S. G. Bayer, R. D. Zumwalde, and K. A. Bursch. 1979. USPHS/NIOSH Membrane Filter Method for Evaluating Airborne Asbestos Fibers. U.S. Department of Health, Education, and Welfare. National Institute for Occupational Safety and Health, Cincinnati, Ohio. 97 pp.

Mueller, P. K., A. E. Alcover, R. L. Stanley, and G. R. Smith. 1975. Asbestos Fiber Atlas. EPA-650/2-75-036, U.S. Environmental Protection Agency, Research Triangle Park, North Carolina. 58 pp.

Ortiz, L. W., and B. L. Isom. 1974. Transfer Technique for Electron Microscopy of Membrane Filter Samples. Amer. Ind. Hyg. Assoc. J. 35(7):423-425.

Samudra, A. V., F. C. Bock, C. F. Harwood, and J. D. Stockham. 1977. Evaluating and Optimizing Electron Microscope Methods for Characterizing Airborne Asbestos. EPA-600/2-78-038, U.S. Environmental Protection Agency, Research Triangle Park, North Carolina. 194 pp.

Samudra, A. V., C. F. Harwood, and J. D. Stockham. 1978. Electron Microscope Measurement of Airborne Asbestos Concentrations: A Provisional Methodology Manual. EPA-600/2-77-178, U.S. Environmental Protection Agency, Research Triangle Park, North Carolina. 57 pp.

Zumwalde, R. D., and J. M. Dement. 1977. Review and Evaluation of Analytical Methods for Environmental Studies of Fibrous Particulate Exposures. DHEW(NIOSH) Publication No. 77-204. National Institute for Occupational Safety and Health, Cincinnati, Ohio. 71 pp.

APPENDIX A

FIGURES

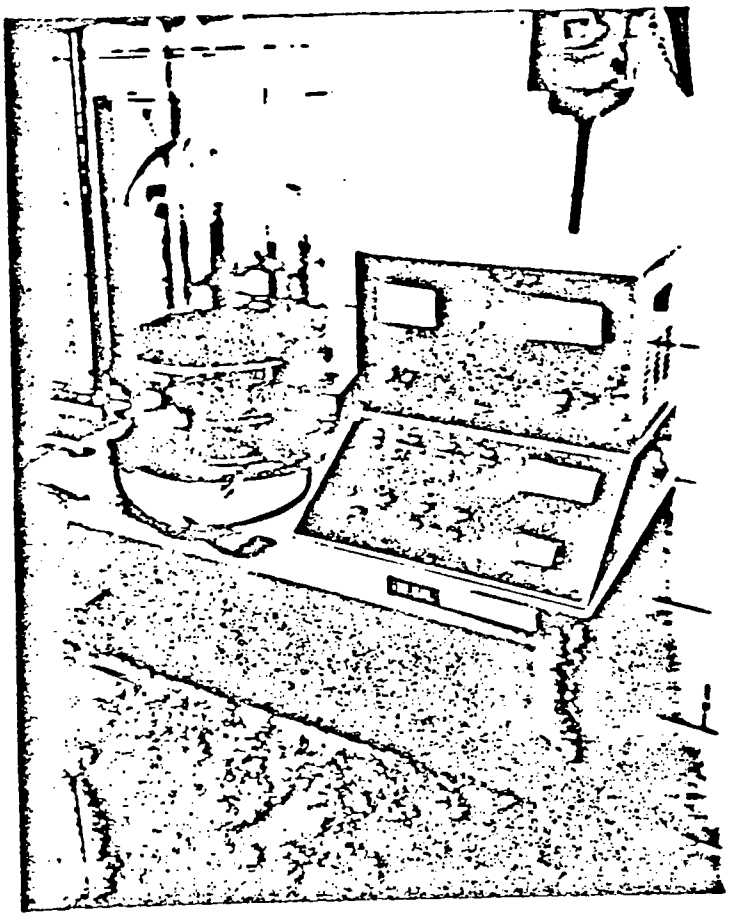

Figure A1. Vacuum evaporator.

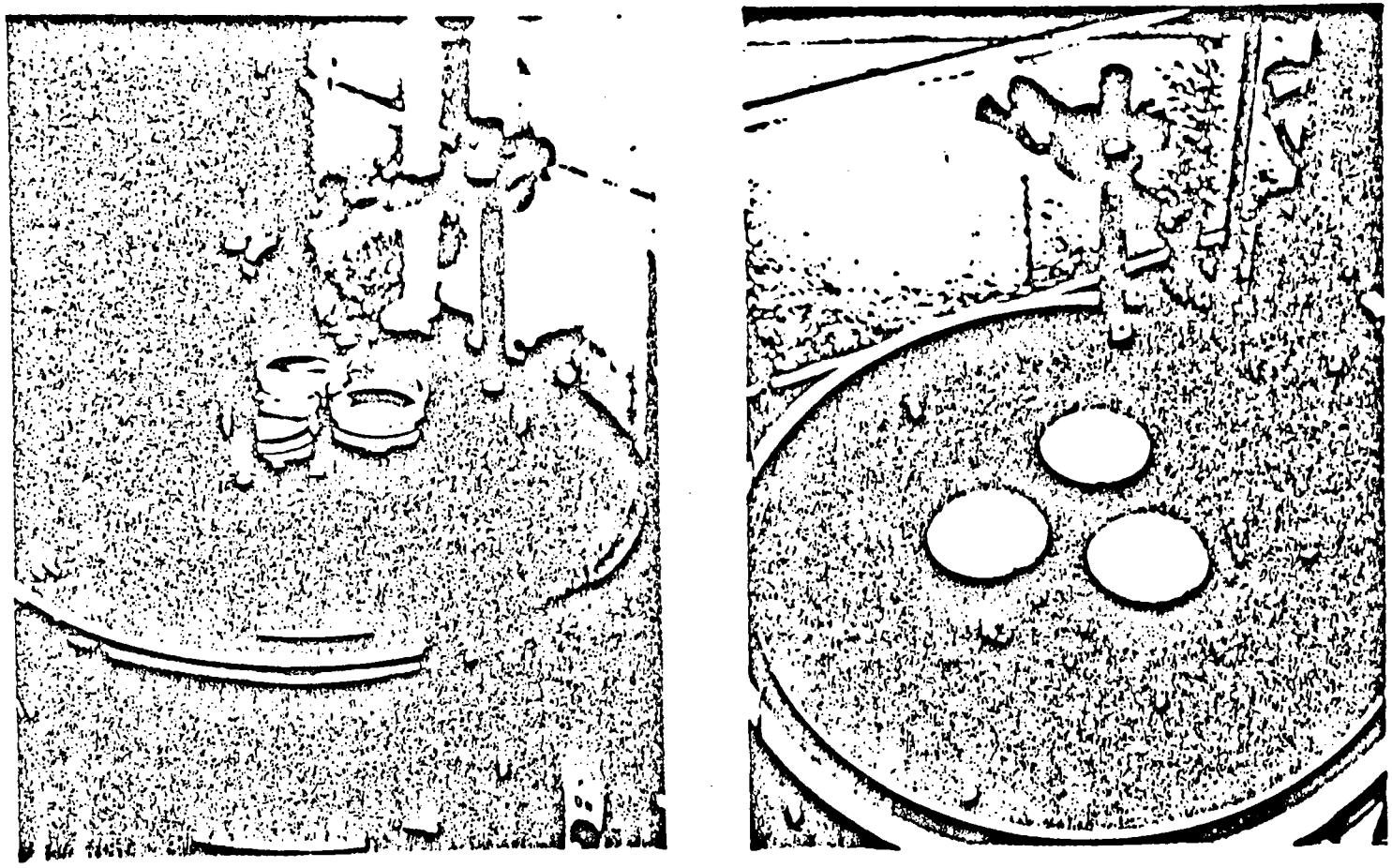

(a) 37-mm diameter.

(b) 47-mm diameter.

Figure A2. Multiple coating arrengement in evaporator.

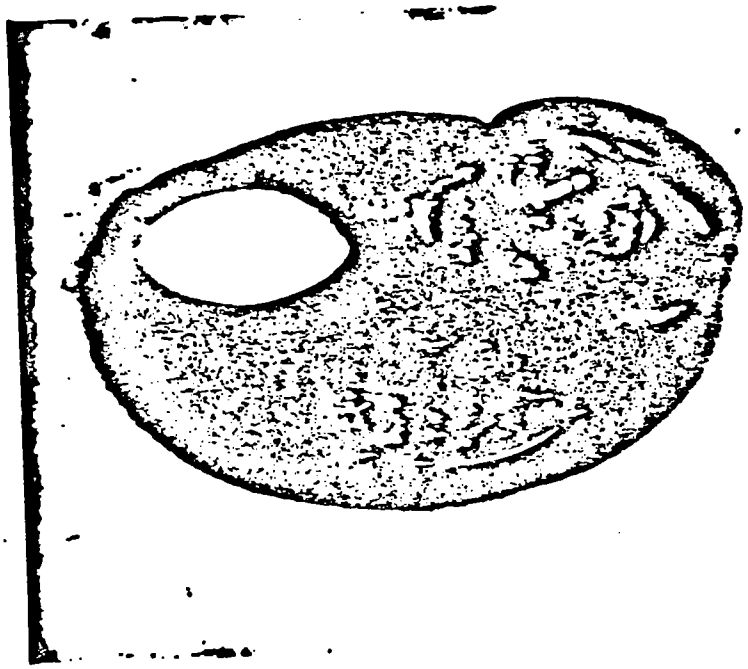

(a) Modified 47-mm-diameter Petri-slides.

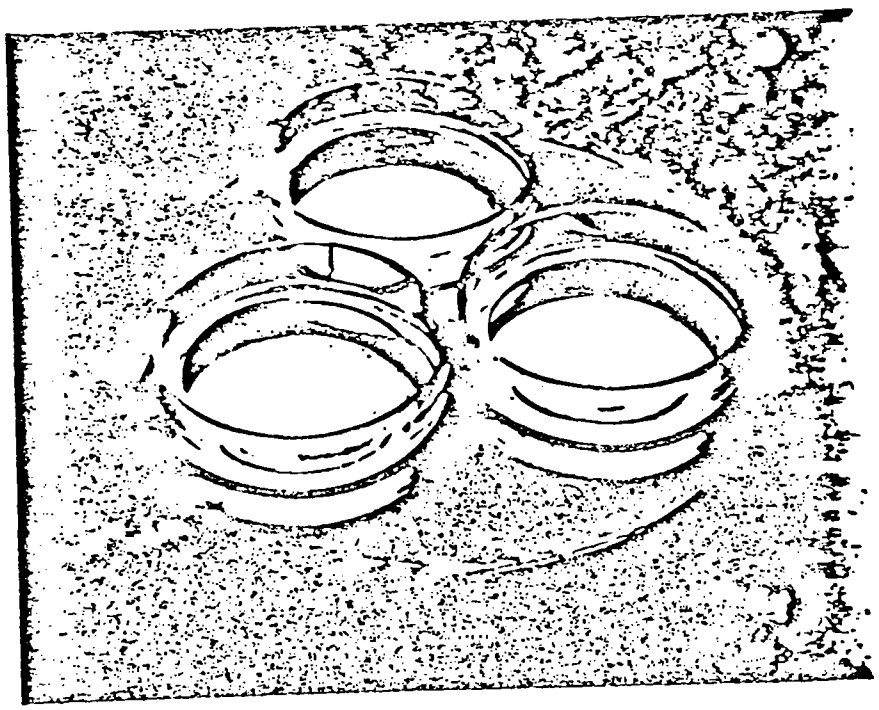

(b) 37-mm-diameter cassette.

Figure A3. Close-up of multiple coating arrangement.

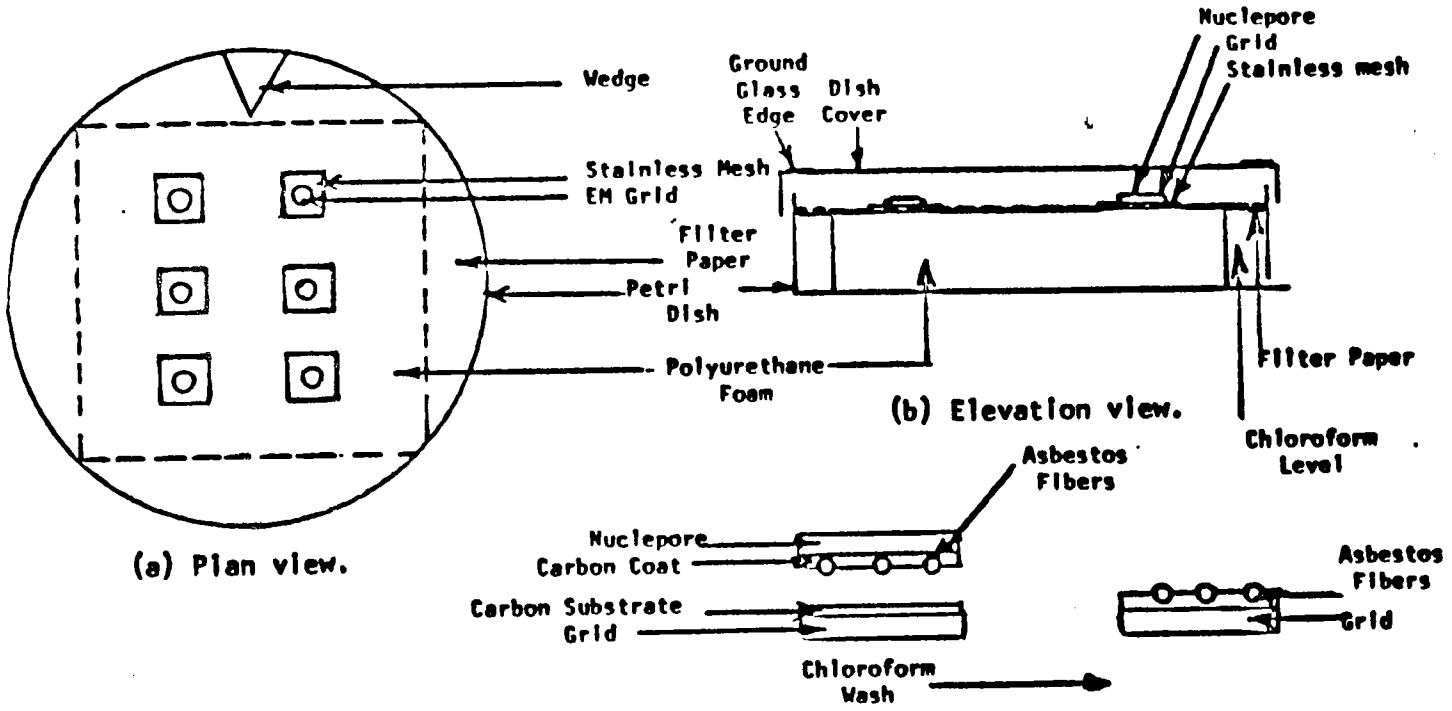

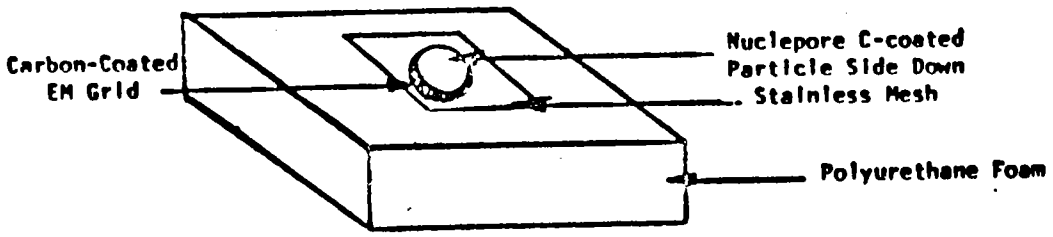

(c) Details of placing the specimen for washing.

Figure A4. Modified Jaffe wick washer method (sketch).

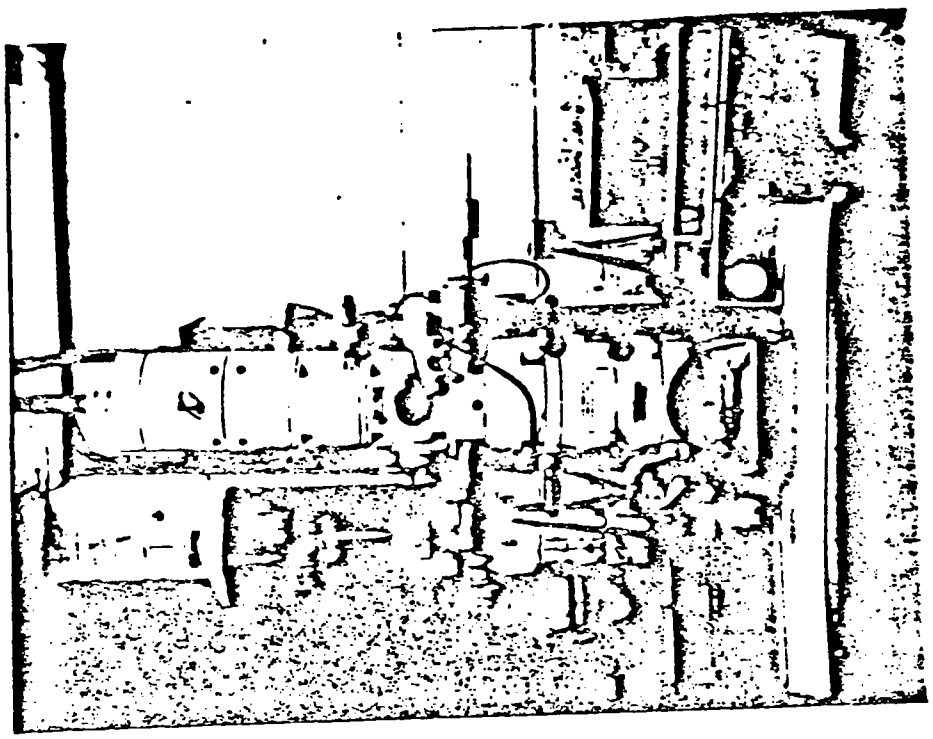

Figure A6. Transmission electron microscope.

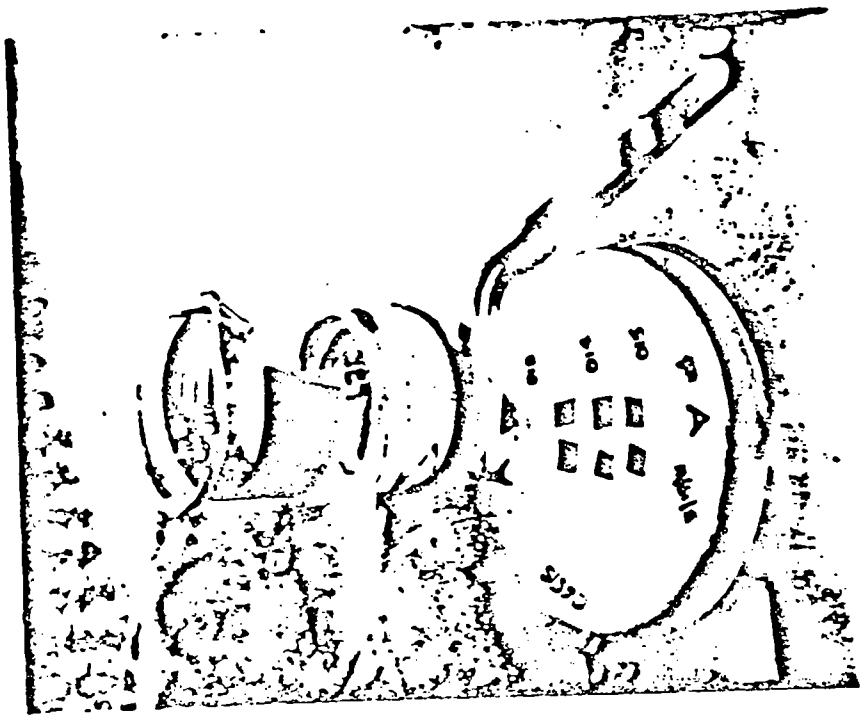

Figure A5. Modified Jaffe wick washer.

Count as one fiber:

Count as two fibers (space between fibers greater than the width of one fiber):

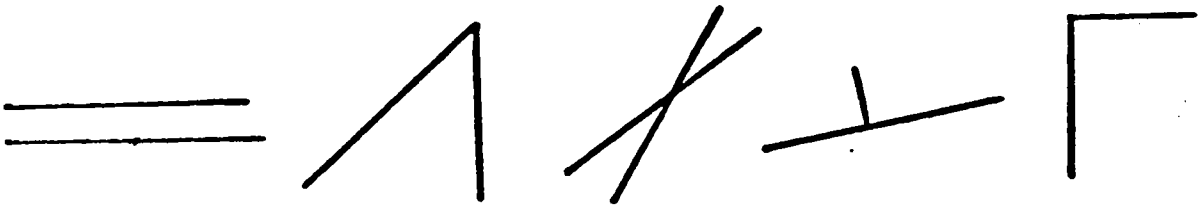

Count as three fibers:

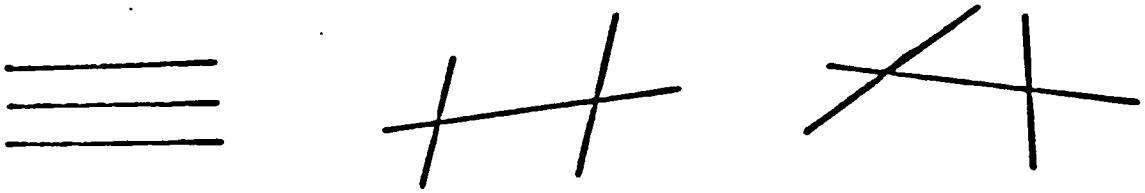

Count as bundles:

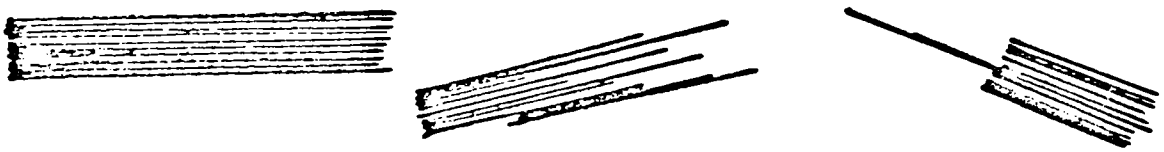

Count as cluster/clump:

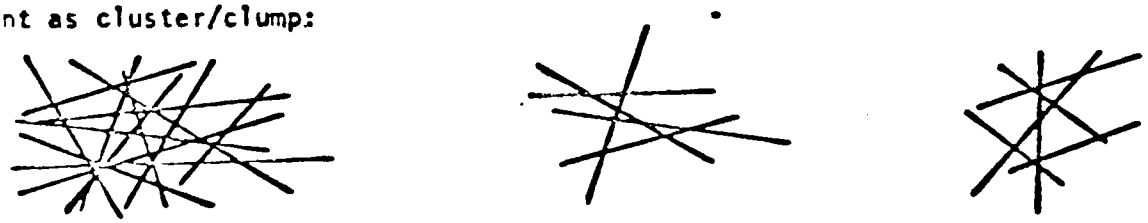

Count as matrix/debris:

Figure A7. Morphology and counting guidelines used in determining asbestos structures.

Sample No. C06470-5-4A1 | Acc. Voltage 100 KV | Date 8/5/81
Filter Type Nuclepore | Beam Current 100 μA | Grid Box B
Filter Area 5.62 cm² | Magnification 20,000 X | Grid Location C-6
Grid Opening Area .0070725 cm² | Comments:

GO	Struct. #	Struct.	Dimension Width	Dimension Length	SAED Observation Chrys	SAED Observation Amph	SAED Observation Ambig	SAED Observation No-ID
1	1	F	1	33	✓			
	2	F	1	19	✓			
	3	F	1	20	✓			
	4	F	1	7			✓	
	5	M	1	9	✓			
	6	B	2	11	✓			
2	7	F	4	20			✓	
	8	F	1	10	✓			
	9	F	1	14	✓			
	10	M	1	6	✓			
	11	M	1	5a	✓			
	12	M	1	25	✓			
	13	M	1	23	✓			
	14	M	1	7			✓	
	15	M	2	12	✓			
	16a	F	1	13	✓			
	17	M	1	6	✓			
3	18	M	1	13				✓
	19	M	1	19			✓	
	20	F	1	17	✓			
	21	M	1	32			✓	
	22	M	1	15			✓	
	23	M	1	15			✓	
4	24	F	1	7				✓
	25	M	3	13	✓			
4	26	M	1	7	✓			
	27	F	1	16				✓
	28	F	1	7	✓			
	29	M	1	26	✓			
	30	M	1	10			✓	
	31	F	1	11				✓
5	32	M	1	41	✓			
	33	B	4	22	✓			
	34	M	1	6	✓			
	35	M	1	6			✓	
	36	M	1	13	✓			
	37	M	1	17				
	38	F	1	29				
	39	M	1	10				
6	40	F	1	24				
	41	B	4	205	✓			
	42	F	5	15		✓		
	43	F	1	11	✓			
	44	F	1	17	✓			
7	45	M	1	9	✓			
	46	F	1	20			✓	
	47	F	1	15	✓			
	48	F	1	13	✓			
	49	F	1	9				✓
	50	F	1	41	✓			

Figure A8. Level I data sheet (example).

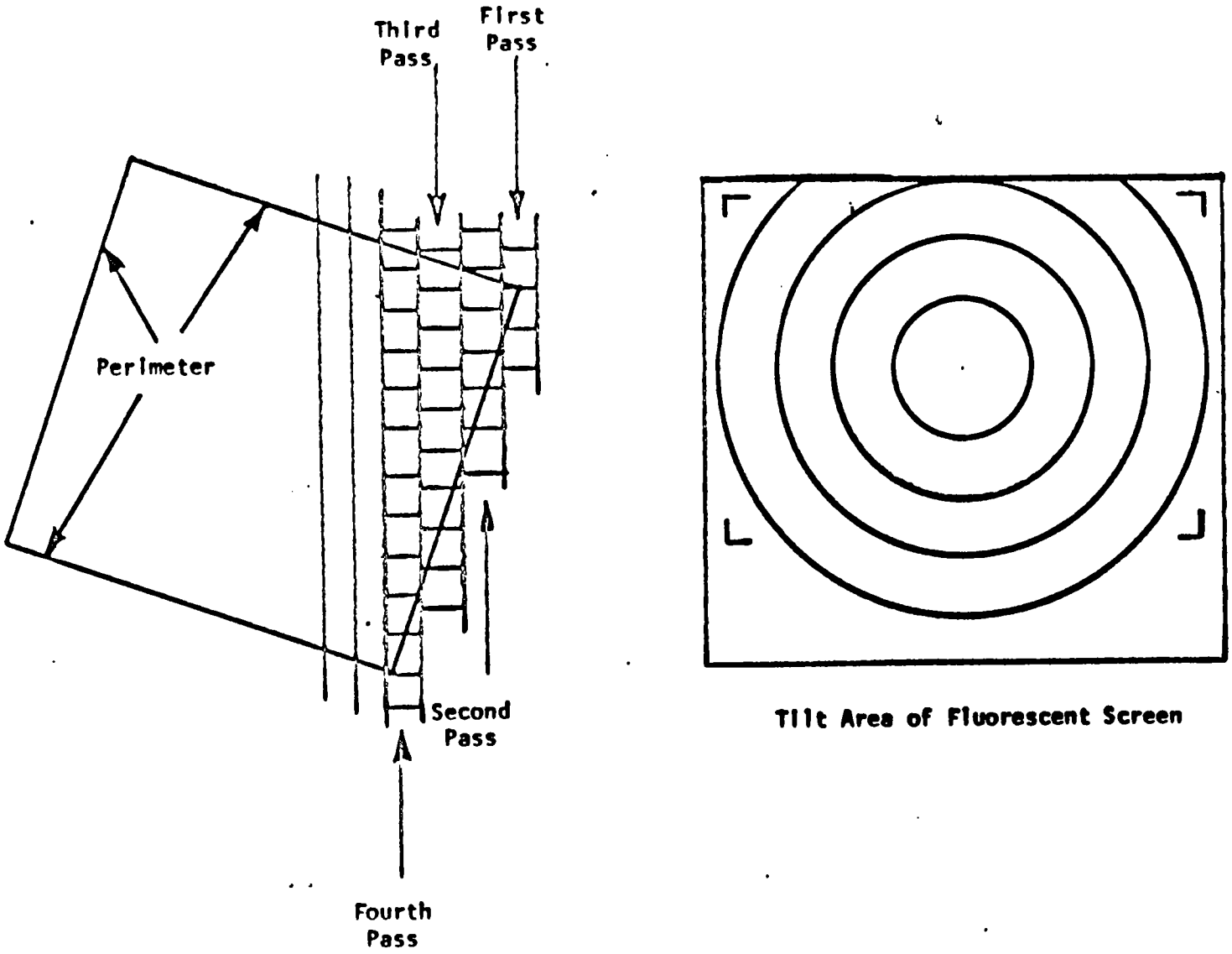

Figure A9. Scanning of full-grid opening.

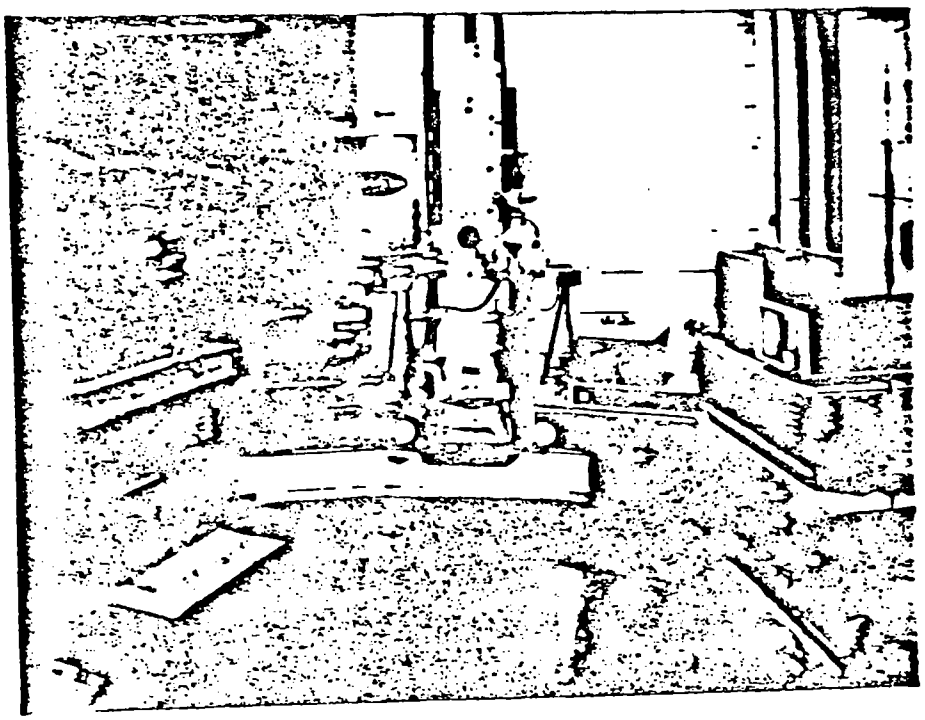

Figure A10. Transmission electron microscope with energy dispersive spectrometer.

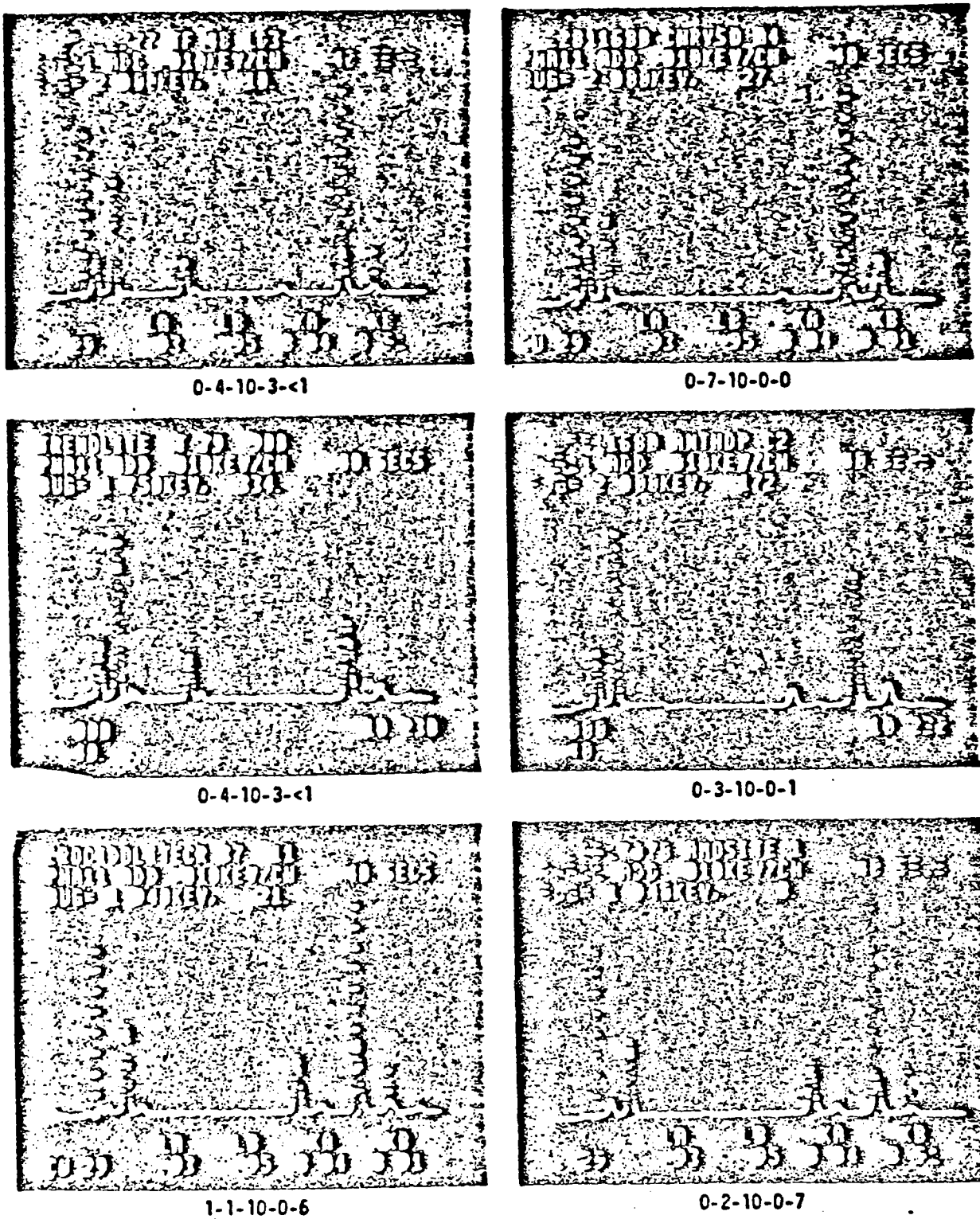

Figure All. Spectra profiles of asbestos standards.

Sample No. C10470-119-6513 EX
Filter Type Nuclepore
Filter Area 9.6 cm^2
Grid Opening Area 72.25×10^{-6} cm^2

Acc. Voltage 100 KV
Beam Current 100 μA
Magnification 20,000 x - Film
Comments Good distribution of particulates - Few extra large particles

Date 4/13/81
Grid Box 2268I
Grid Location D-7

GO	Struct. #	Struct.	Dimension Width	Dimension Length	SAED Observation Chyrs	Amph	Ambig	Non-A	No-P	SAED/Image 0°	EDS Na	Mg	Si	Ca	Fe	ID
1	1	F	2	26		✓					—	9	19	7	7	TR
	2	"	9	30		✓										
2	0	"														
3	3		10	85		✓					—	35	110	35	17	TR
	4	"	6	65		✓					—	19	59	22	21	TR
4	5	"	4	23		✓					—	66	152	—	28	AN
5	6	"	1	8				✓								
	7	"	3	48		✓	(✓)				—	57	170	43	16	TR
6	8	"	2	30				✓								
7	9	"	2	11				✓								✓
	10	"	15	80				✓								✓
	11	"	10	80				✓								✓
	12	"	5	45				✓								✓
8	13	"	6	43			(✓)	✓								✓
	14	"	3	25		✓	(✓)				—	15	51	18	6	TR
9	15	"	7	26				✓								
10	16	"	4	25				✓								
	17	"	4	38				✓								

Figure A12. Level II data sheet (example).

EM DATA REPORT

Sample Number: R09-2865 Date Analyzed: 3/26/81
IITRI Sample No.: C010-1859 Date Sample Received: 1/30/81
Sample Type: Bulk, Air, Water, Misc. (circle one)
Filter Type: Nuclepore Area of Filter Deposit (cm^2): 8.6
Volume of Fluid Sampled: NA Mass Deposited: NA

1. Total Number of Structures: 101
2. Total Number of Asbestos Structures: 93
   - 2.1 Chrysotile 88
   - 2.2 Amphibole 5
     - Crocidolite 5 Anthophyllite
     - Tremolite Actinolite
     - Amosite Non-Identity
   - 2.3 Non-Identity 8
3. Asbestos Structure Description
   - 3.1 Total Number of Fibers: 85 Mass (ng) .0016
     - 3.1.1 Chrysotile 80 Mass (ng) .0010
       - Fiber Length; Range (μm) .31 - 2.25 Mean (μm) 0.78
       - Fiber Diameter; Range (μm) .06 - .25 Mean (μm) 0.07
       - Aspect Ratio; Range (μm) 3.5 - 31.0 Mean (μm) 11.00
     - 3.2.2 Amphibole 5 Mass (ng) .0006
       - Fiber Length; Range (μm) .31 - 2.19 Mean (μm) 1.00
       - Fiber Diameter; Range (μm) .06 - .31 Mean (μm) 0.15
       - Aspect Ratio; Range (μm) 5.0 - 10.0 Mean (μm) 6.40
   - 3.2 Total Number of Bundles: 5 ,Mass (ng) .0007
   - 3.3 Total Number of Clusters/Clumps: 2 ,Mass (ng) .0002
   - 3.4 Total Number of Matrix/Debris: 1 ,Mass (ng) negligible
4. Area of Filter Sample Analyzed, (cm^2): .0007225
5. Total Mass of Asbestos Analyzed (ng): .0025
6. Number of Pictures Attached: 2
7. Qualitative Description of Non-Asbestos Particles Few, small particles--non-descriptive
8. Comments: Particulate loading OK.

Figure A13. EM data report (example).

SAMPLE SUMMARY REPORT

Sample Number: R09-2865 Date of Report: 4/1/81
IITRI Sample No.: C010-1859 Date Sample Received: 1/30/81
Sample Type: Bulk, (Air,) Water, Misc. (circle one)
Filter Type: Nuclepore Area of Filter Deposit (cm^2): 8.6
Volume of Fluid Sampled: NA Mass Deposited: NA

1. Total Number of Structures: 1,202,215
2. Total Number of Asbestos Structures: 1,106,990
   - 2.1 Chrysotile 1,047,474
   - 2.2 Amphibole 59,516
     - Crocidolite 59,516
     - Anthophyllite
     - Tremolite
     - Actinolite
     - Amosite
     - Non-Identity
   - 2.3 Non-Identity 95,225
3. Asbestos Structure Description
   - 3.1 Total Number of Fibers: 1,011,765 Mass (ng) 19.00
     - 3.1.1 Chrysotile 952,249 Mass (ng) 11.90
       - Fiber Length; Range (um) .31 - 2.25 Mean (um) 0.78
       - Fiber Diameter; Range (um) .06 - .25 Mean (um) 0.07
       - Aspect Ratio; Range (um) 3.5 - 31.0 Mean (um) 11.00
     - 3.2.2 Amphibole 59,516 Mass (ng) 7.14
       - Fiber Length; Range (um) .31 - 2.19 Mean (um) 1.00
       - Fiber Diameter; Range (um) .06 - .31 Mean (um) 0.15
       - Aspect Ratio; Range (um) 5.0 - 10.0 Mean (um) 6.40
   - 3.2 Total Number of Bundles: 59,516 ,Mass (ng) 8.30
   - 3.3 Total Number of Clusters/Clumps: 23,806 ,Mass (ng) 2.10
   - 3.4 Total Number of Matrix/Debris: 11,903 ,Mass (ng) 0.10
4. Area of Filter Sample Analyzed, (cm^2): .0007225
5. Total Mass of Asbestos Analyzed (ng): 29.5
6. Number of Pictures Attached: 2
7. Qualitative Description of Non-Asbestos Particles Few, small particles--Non-descriptive
8. Comments: Particulate loading OK.

Figure A14. Sample summary report (example).

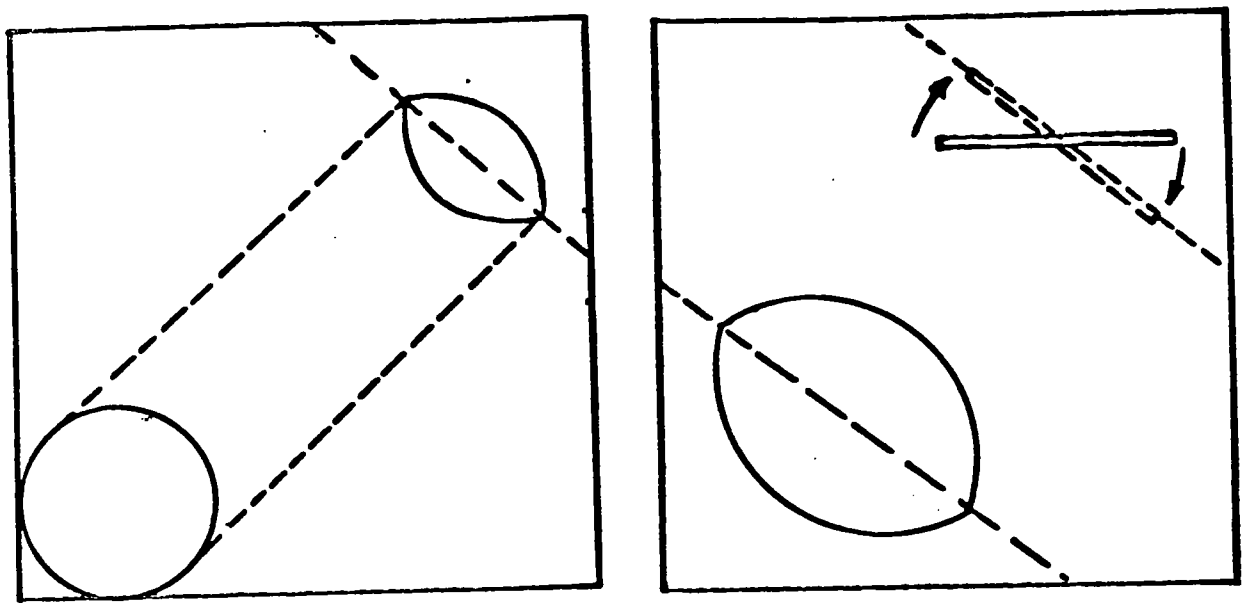

(a) Effects of tilting.

(b) Fiber alignment.

Figure A15. Effects of tilting and alignment of fiber.

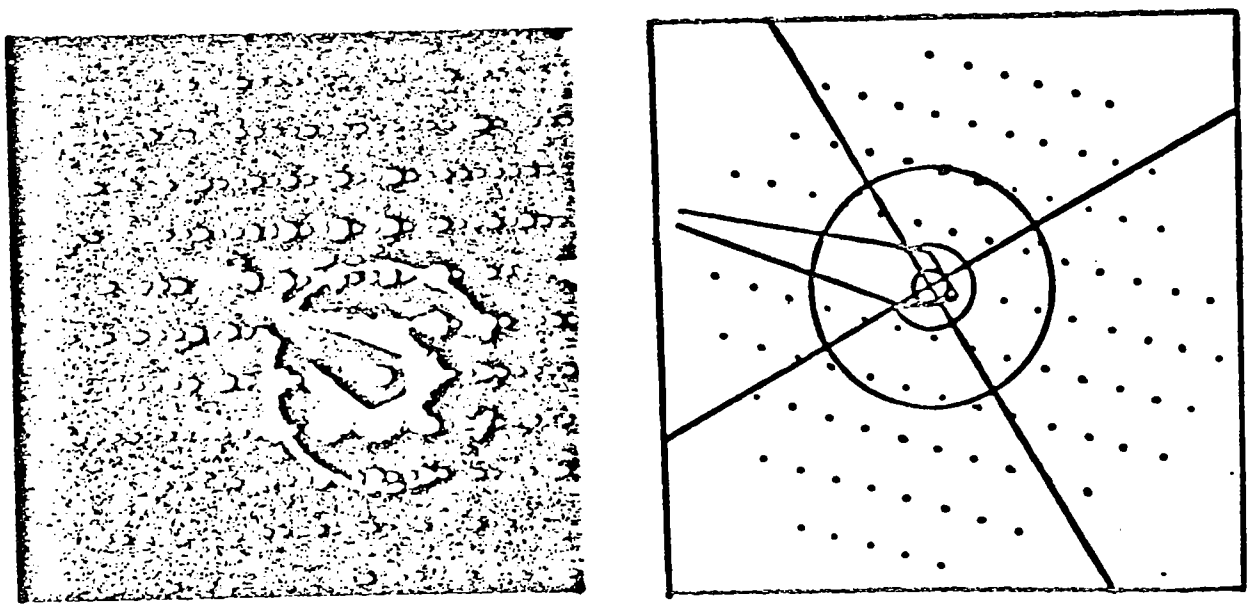

Figure A16. Method of measuring two perpendicular diameters for each ring.

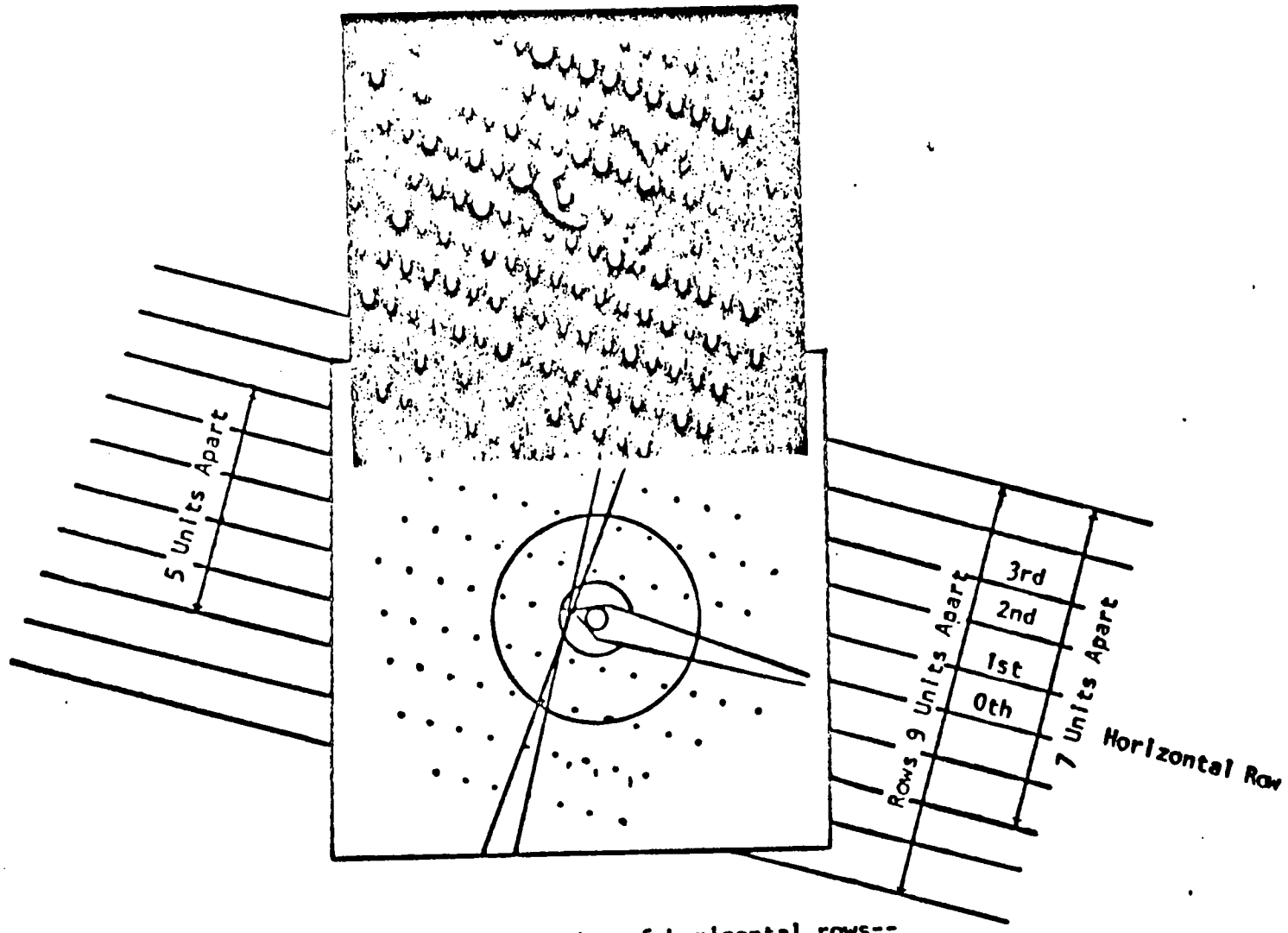

Figure A17. Method of recognizing a horizontal row of spots.

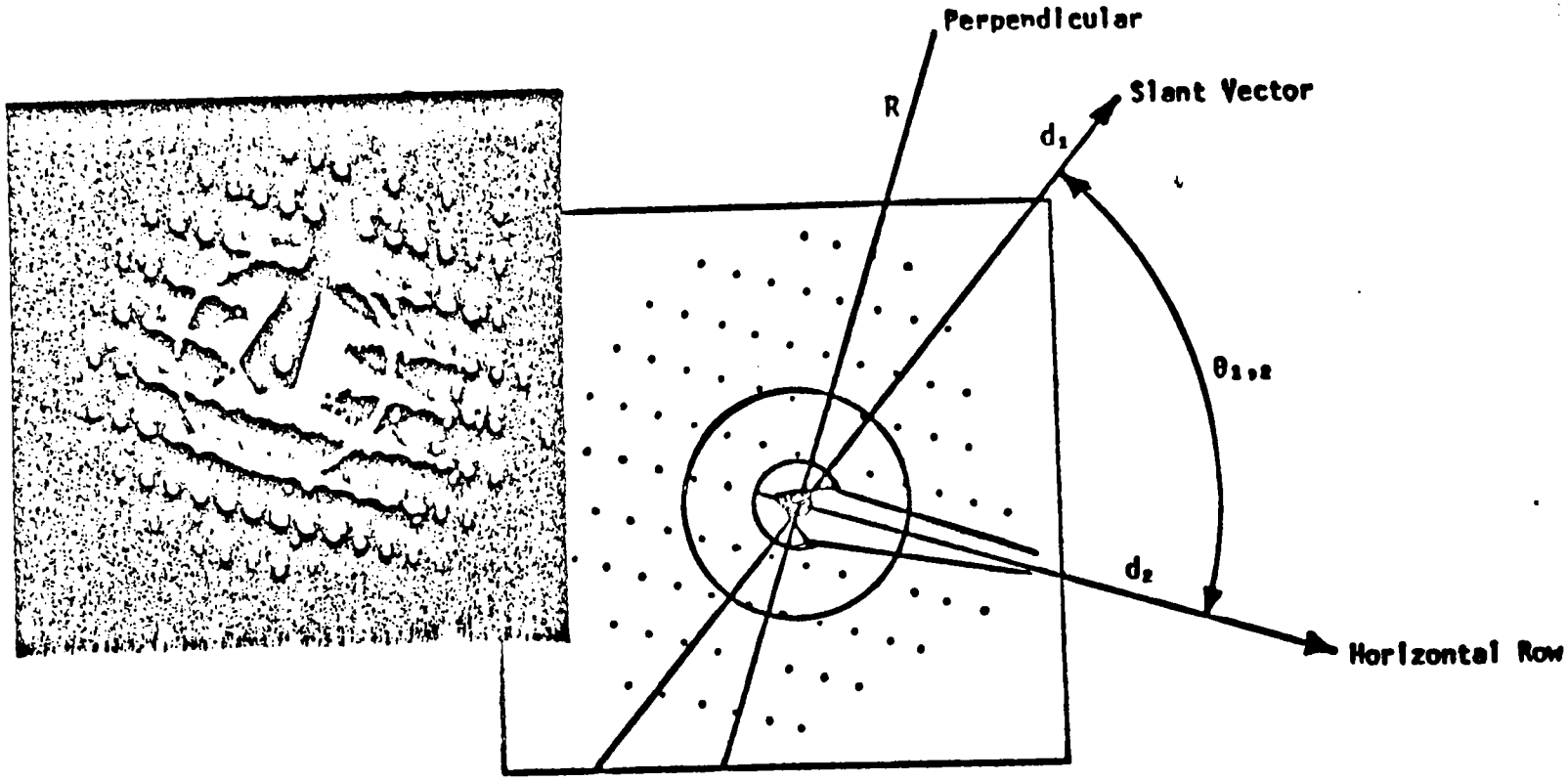

Draw the 0th horizontal row.

Draw a perpendicular through the origin.

Join the origin to the first spot to the right of the perpendicular in the 1st row and extend the line to measure the acute angle θ of this line from the 0th row.

Figure A18. Relationship of d_1, d_2, $\theta_{1,2}$, and R.

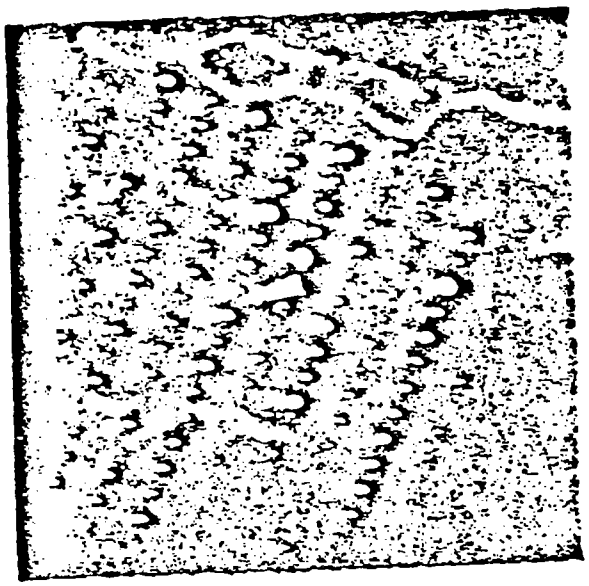

(a) Zone axis [100].

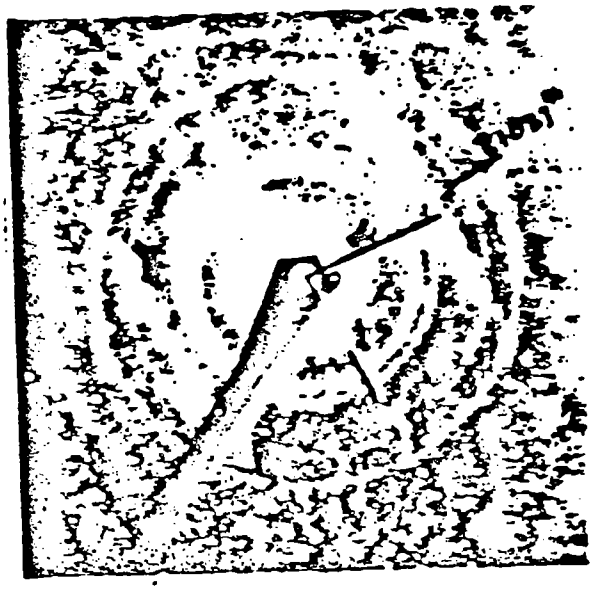

(b) Zone axis [30$\bar{1}$].

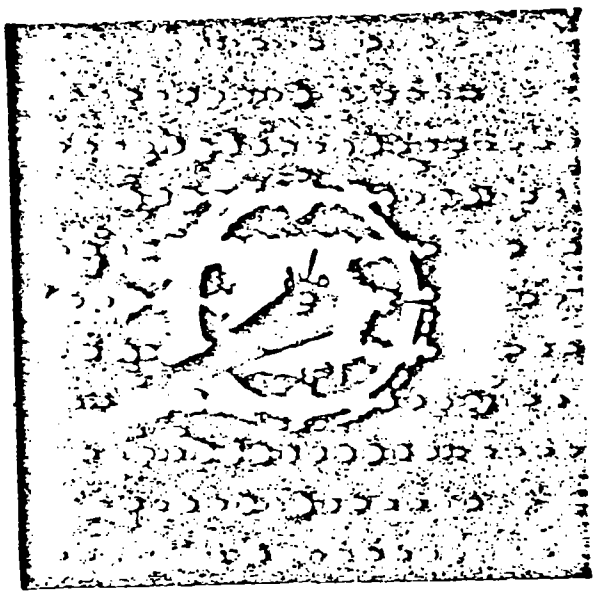

(c) Zone axis [101].

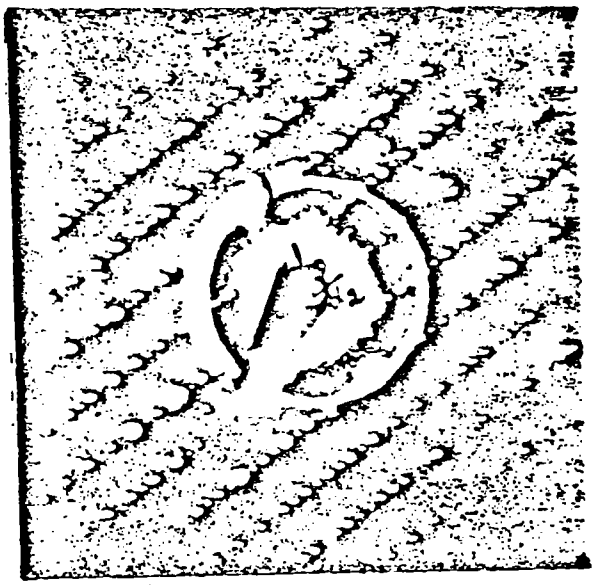

(d) Zone axis [$\bar{1}$01].

Figure A19. Typical Zone-axis SAED patterns from amosite standard specimen. (Jones et al., 1981)

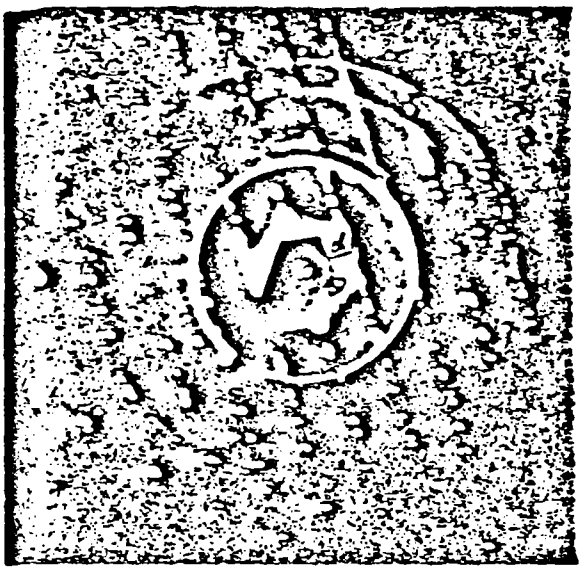

(a) Zone axis [100].

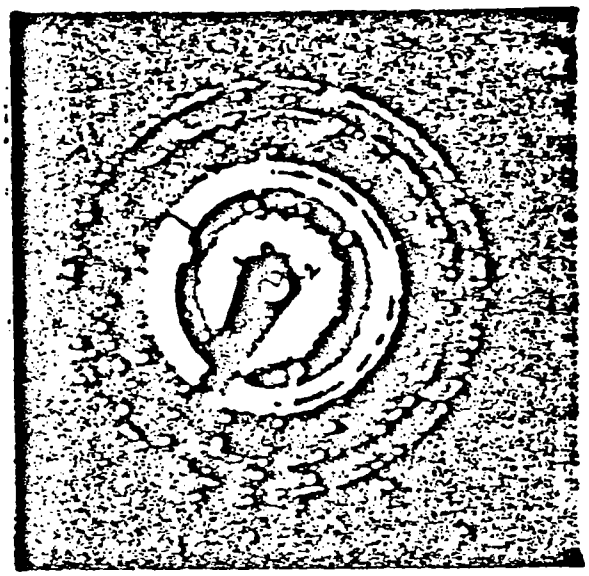

(b) Zone axis [101].

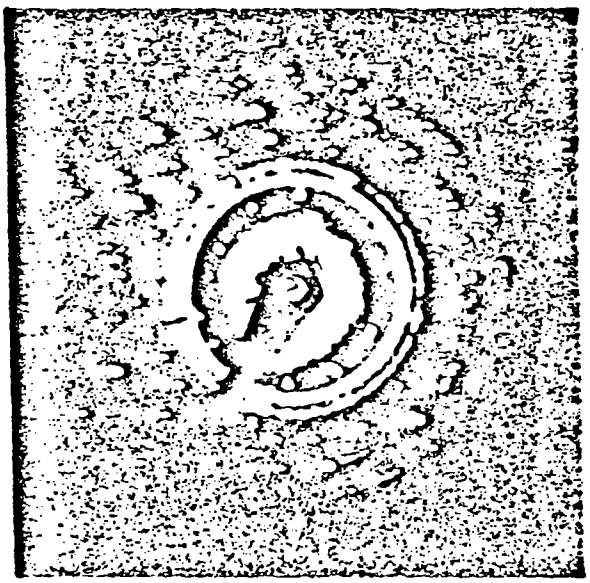

(c) Zone axis [$\bar{1}$10].

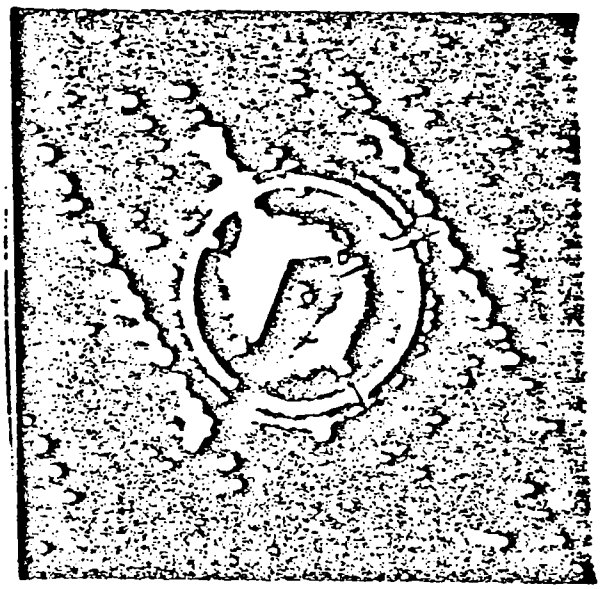

(d) Zone axis [30$\bar{1}$].

Figure A20. Typical zone-axis patterns from crocidolite standard specimen. (Jones et al., 1981)

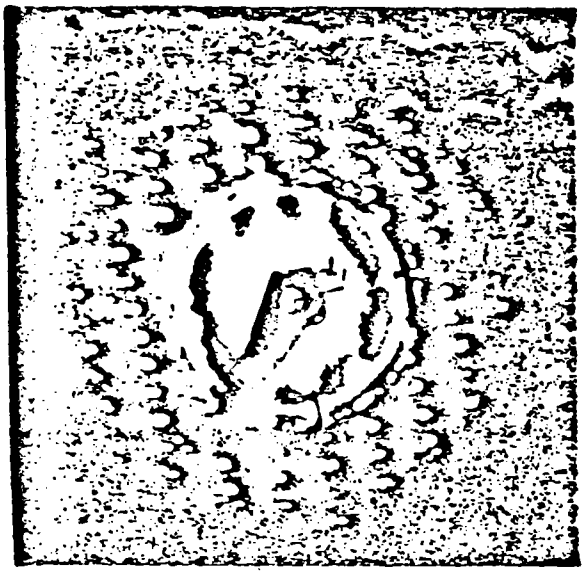

(a) Zone axis [100].

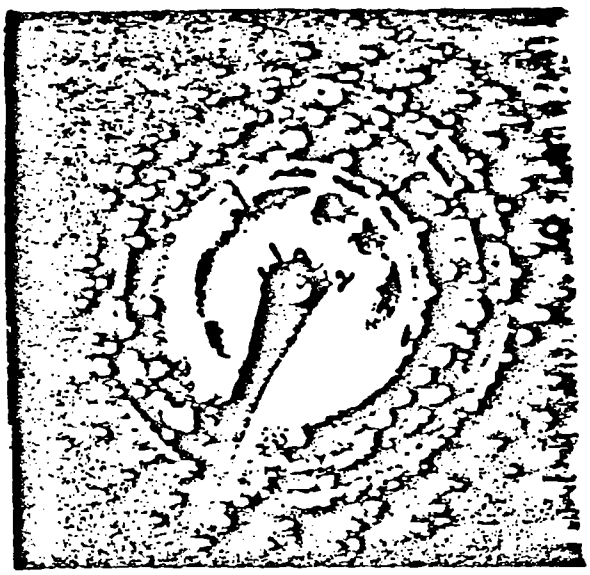

(b) Zone axis [10$\bar{1}$].

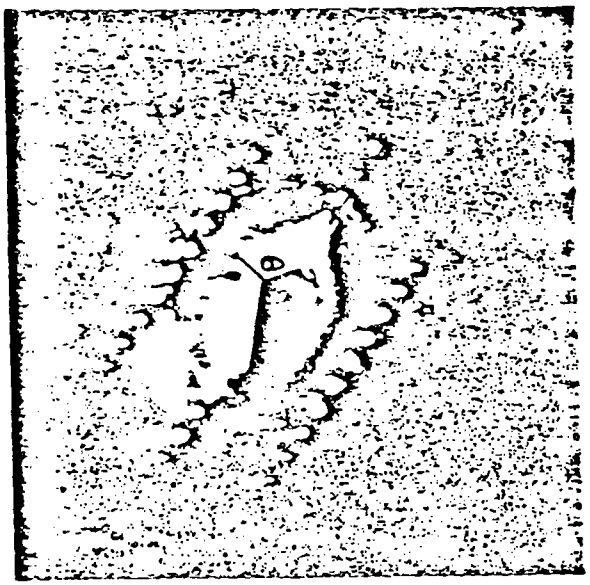

(c) Zone axis [$\bar{2}$0$\bar{1}$].

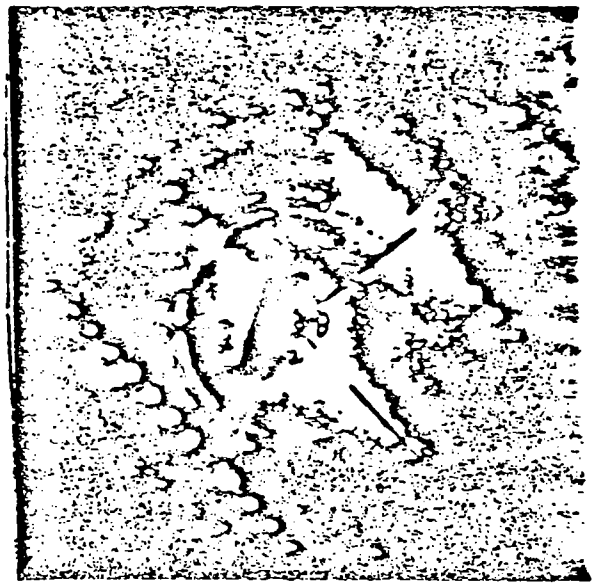

(d) Zone axis [30$\bar{1}$].

Figure A21. Typical zone-axis patterns from tremolite standard specimen. (Jones et al., 1981)

(a) Zone axis [100].

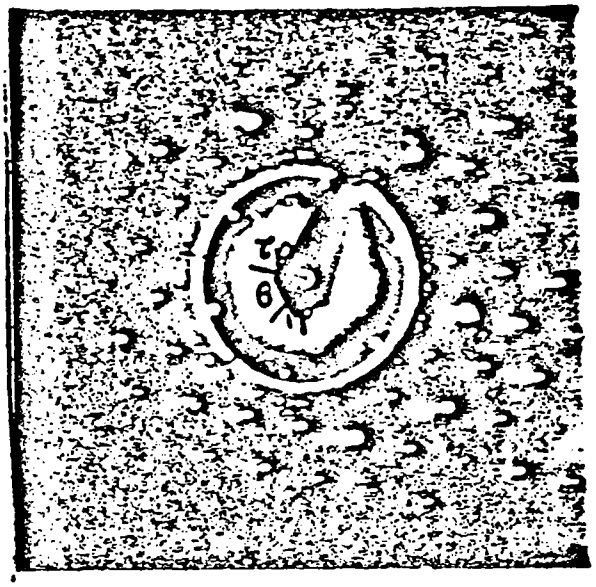

(b) Zone axis [$\bar{1}42$].

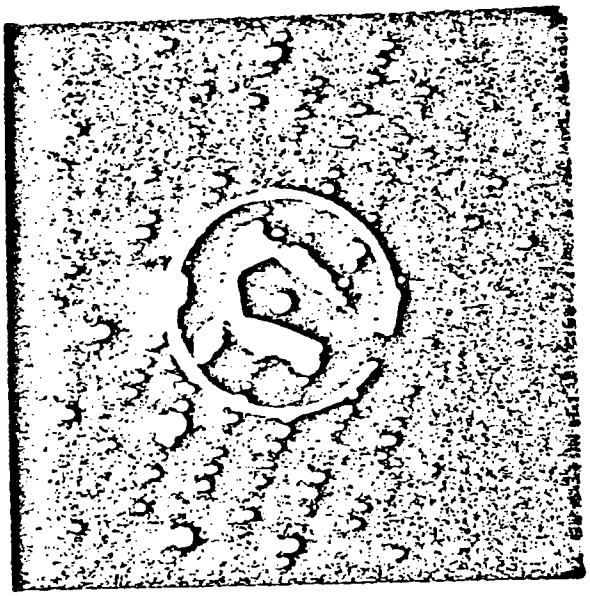

(c) Commonly observed orientation.

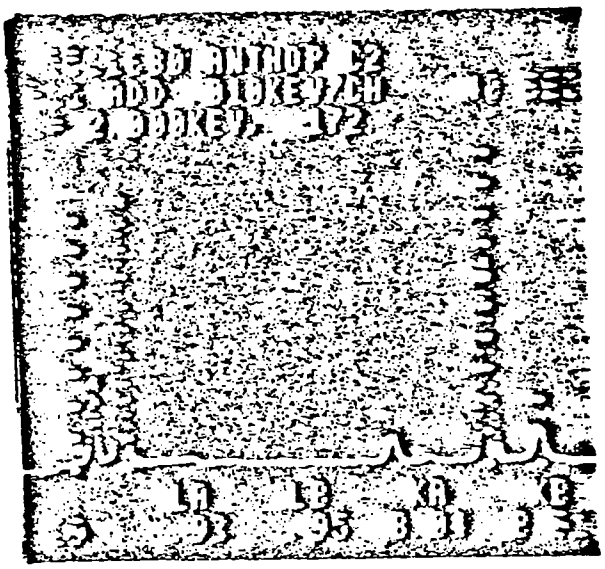

(d) EDAX.

Figure A22. Typical SAED patterns and EDAX spectra from anthophyllite standard specimen. (Jones et al., 1981)

APPENDIX B

COMPUTER PRINTOUT OF LEVEL I ANALYSIS (EXAMPLE)

ITT RESEARCH INSTITUTE STRUCTURE ANALYSIS DATA
INDIVIDUAL OBJECT DATA TABLE (F=FIBER, B=BUNDLE, C=CLUSTER, M=MATRIX)
TABLE PREPARATION DATE: 21-APR-81

SAMPLE CODE:

Grd Opn	Obj	Str	Size (Micron) Depth	Width	Length	Ratio	Mass (Picogram) Chrysotile	Amphibole	Ambis	Not Asbe	No Patt	X-Rev
.1	1	F	0.000	0.187	1.38	7.3	.	.	.	X	.	
1	2	F	0.000	0.125	0.75	6.0	.	.	.	X	.	
2	3	F	0.000	0.500	8.12	16.3	.	4.786	.	.	.	
2	4	F	0.000	0.437	2.81	6.4	.	1.268	.	.	.	
2	5	F	0.000	0.250	0.94	3.7	.	.	.	X	.	
3	6	F	0.000	0.375	2.19	5.8	.	.	.	X	.	
3	7	F	0.000	0.750	3.25	4.3	.	4.307	.	.	.	
3	8	F	0.000	0.625	7.81	12.5	.	.	.	X	.	
4	9	F	0.000	0.937	3.00	3.2	.	.	.	X	.	
4	10	F	0.000	0.125	1.25	10.0	.	0.046	.	.	.	
7	11	F	0.000	0.250	9.37	37.5	.	1.380	.	.	.	
7	12	F	0.000	0.812	6.00	7.4	.	.	.	X	.	
7	13	F	0.000	0.312	3.63	11.6	.	.	.	X	.	
8	14	F	0.000	0.625	5.94	9.5	.	5.464	.	.	.	
8	15	F	0.000	0.625	3.12	5.0	.	.	.	X	.	
9	16	F	0.000	0.250	2.50	10.0	.	.	.	X	.	
12	17	F	0.000	0.187	0.94	5.0	.	.	.	X	.	
12	18	F	0.000	0.625	3.44	5.5	.	3.164	.	.	.	
12	19	F	0.000	0.312	1.87	6.0	.	.	.	X	.	
13	20	F	0.000	0.187	1.00	5.3	.	0.083	.	.	.	
13	21	F	0.000	0.437	3.88	8.9	.	.	.	X	.	
13	22	F	0.000	0.312	5.00	16.0	.	1.150	.	.	.	
14	23	F	0.000	0.562	3.06	5.4	.	.	.	X	.	
14	24	F	0.000	0.062	0.69	11.0	.	.	.	X	.	
14	25	F	0.000	0.187	3.38	18.0	.	0.280	.	.	.	
15	26	F	0.000	1.562	5.00	3.2	.	.	.	X	.	
15	27	F	0.000	0.937	3.75	4.0	.	.	.	X	.	
16	28	F	0.000	0.750	6.38	8.5	.	.	.	X	.	
16	29	F	0.000	0.250	1.56	6.2	.	.	.	X	.	

APPENDIX B (Continued)

IIT RESEARCH INSTITUTE STRUCTURE ANALYSIS DATA
SINGLE SAMPLE SUMMARY TABLES
SAMPLE CODE: TABLE PREPARATION DATE: 21-APR-01

Aerosol Object Count And Calculated Object Mass Characteristics

Object Structure	Type	Actual Object Count	Number Concen. (Number Per Cu M)	Mass Concen. (Picogram Per Cu M)	Average Width (Micron)	Average Length (Micron)	Average Length To Width Ratio
Fiber	Chrysotile	0.	0.	0.0	0.00 ± 0.00	0.00 ± 0.00	0.00 ± 0.00
	Amphibole	12.	8304.	19155.4	0.38 ± 0.21	5.20 ± 4.50	15.55 ±13.02
	Other	22.	15225.		0.46 ± 0.37	2.87 ± 1.96	7.81 ± 5.03
	All Fiber	34.	23529.		0.43 ± 0.32	3.69 ± 3.24	10.47 ± 9.27

Sample Collection and Preparation Data

Air Volume	=	1.00 Cu M
Deposit Area	=	1.00 Sq Cm
Ashed Area	=	1.00 Sq Cm
Redeposit Area	=	1.00 Sq Cm

Grid Data

Grid ID: 22501/B-8,B-9
Individual Grid Opening = 0.000072 Sq Cm
Number of Grid Openings = 20
Film Magnification = 20000

APPENDIX B (Continued)

IIT RESEARCH INSTITUTE STRUCTURE ANALYSIS DATA
INDIVIDUAL OBJECT DATA TABLE (F=FIBER, B=BUNDLE, C=CLUSTER, M=MATRIX)
TABLE PREPARATION DATE: 21-APR-01

SAMPLE CODE:

Grd Opn	Obj	Str	Size (Micron) Depth	Width	Length	Ratio	Mass (Picogram) Chrysotile	Amphibole	Ambig	Not Asbe	No Patt	X-Ray
16	30	F	0.000	0.375	16.88	45.0	.	5.591	.	.	.	
17	31	F	0.000	0.250	1.56	6.2	.	.	.	X	.	
19	32	F	0.000	0.187	1.44	7.7	.	.	.	X	.	
19	33	F	0.000	0.062	1.69	27.0	.	0.160	.	.	.	
19	34	F	0.000	0.187	1.94	10.3	.		.	.	.	
			Total Mass (Picogram)=				0.000	27.680				
			Total Count =				0.	12.	0.	22.	0.	

APPENDIX C

COMPUTER PRINTOUT OF LEVEL II ANALYSIS (EXAMPLE)

IIT RESEARCH INSTITUTE STRUCTURE ANALYSIS DATA
INDIVIDUAL OBJECT DATA TABLE (F=FIBER, B=BUNDLE, C=CLUSTER, M=MATRIX)
TABLE PREPARATION DATE: 21-APR-81

SAMPLE CODE:

Grd Opn	Obj	Str	Size (Micron) Depth	Width	Length	Ratio	Mass (Picogram) Chrysotile	Amphibole	Ambig	Not Asbe	No Patt	X-Ray
1	1	F	0.000	0.125	1.63	13.0	.	0.0598	.	.	.	MG(9) SI(19) CA(7) FE(7)
1	2	F	0.000	0.562	1.87	3.3	.	1.3977	.	.	.	TCGW
3	3	F	0.000	0.625	5.31	8.5	.	4.8892	.	.	.	MG(35) SI(110) CA(35) FE(17)
3	4	F	0.000	0.375	4.06	10.8	.	1.3460	.	.	.	MG(19) SI(59) CA(22) FE(21)
4	5	F	0.000	0.250	1.44	5.8	.	0.2117	.	.	.	MG(66) SI(152) FE(28)
5	6	F	0.000	0.062	0.50	8.0	.	.	.	X	.	
5	7	F	0.000	0.187	3.00	16.0	.	0.2485	.	.	.	MG(57) SI(170) CA(43) FE(16)
6	8	F	0.000	0.125	1.87	15.0	.	.	.	X	.	
7	9	F	0.000	0.125	0.69	5.5	.	.	.	X	.	
7	10	F	0.000	0.937	5.00	5.3	.	.	.	X	.	
7	11	F	0.000	0.625	5.00	8.0	.	.	.	X	.	
7	12	F	0.000	0.312	2.81	9.0	.	.	.	X	.	
8	13	F	0.000	0.375	2.69	7.2	.	.	.	X	.	
8	14	F	0.000	0.187	1.56	8.3	.	0.1294	.	.	.	MG(15) SI(51) CA(18) FE(6)
9	15	F	0.000	0.437	1.63	3.7	.	.	.	X	.	
10	16	F	0.000	0.250	1.56	6.2	.	.	.	X	.	
10	17	F	0.000	0.250	2.38	9.5	.	.	.	X	.	
			Total Mass (Picogram)=				0.0000	0.2822				
			Total Count =				0.	7.	0.	10.	0.	

IIT RESEARCH INSTITUTE STRUCTURE ANALYSIS DATA
SINGLE SAMPLE SUMMARY TABLES
SAMPLE CODE:
TABLE PREPARATION DATE: 21-APR-81

Aerosol Object Count And Calculated Object Mass Characteristics

Object Structure	Type	Actual Object Count	Number Concen. (Number Per Cu M)	Mass Concen. (Picogram Per Cu M)	Average Width (Micron)	Average Length (Micron)	Average Length To Width Ratio
Fiber	Chrysotile	0.	0.	0.0	0.00 ± 0.00	0.00 ± 0.00	0.00 ± 0.00
	Amphibole	7.	9689.	11463.3	0.33 ± 0.20	2.70 ± 1.50	9.39 ± 4.29
	Other	10.	13841.		0.35 ± 0.27	2.41 ± 1.56	7.75 ± 3.11
	All Fiber	17.	23529.		0.34 ± 0.23	2.53 ± 1.49	8.42 ± 3.61

Sample Collection and Preparation Data

Air Volume = 1.00 Cu M
Deposit Area = 1.00 Sq Cm
Ashed Area = 1.00 Sq Cm
Redeposit Area = 1.00 Sq Cm

Grid Data

Grid ID: 22581/D-7
Individual Grid Opening = 0.000072 Sq Cm
Number of Grid Openings = 10
Film Magnification = 20000